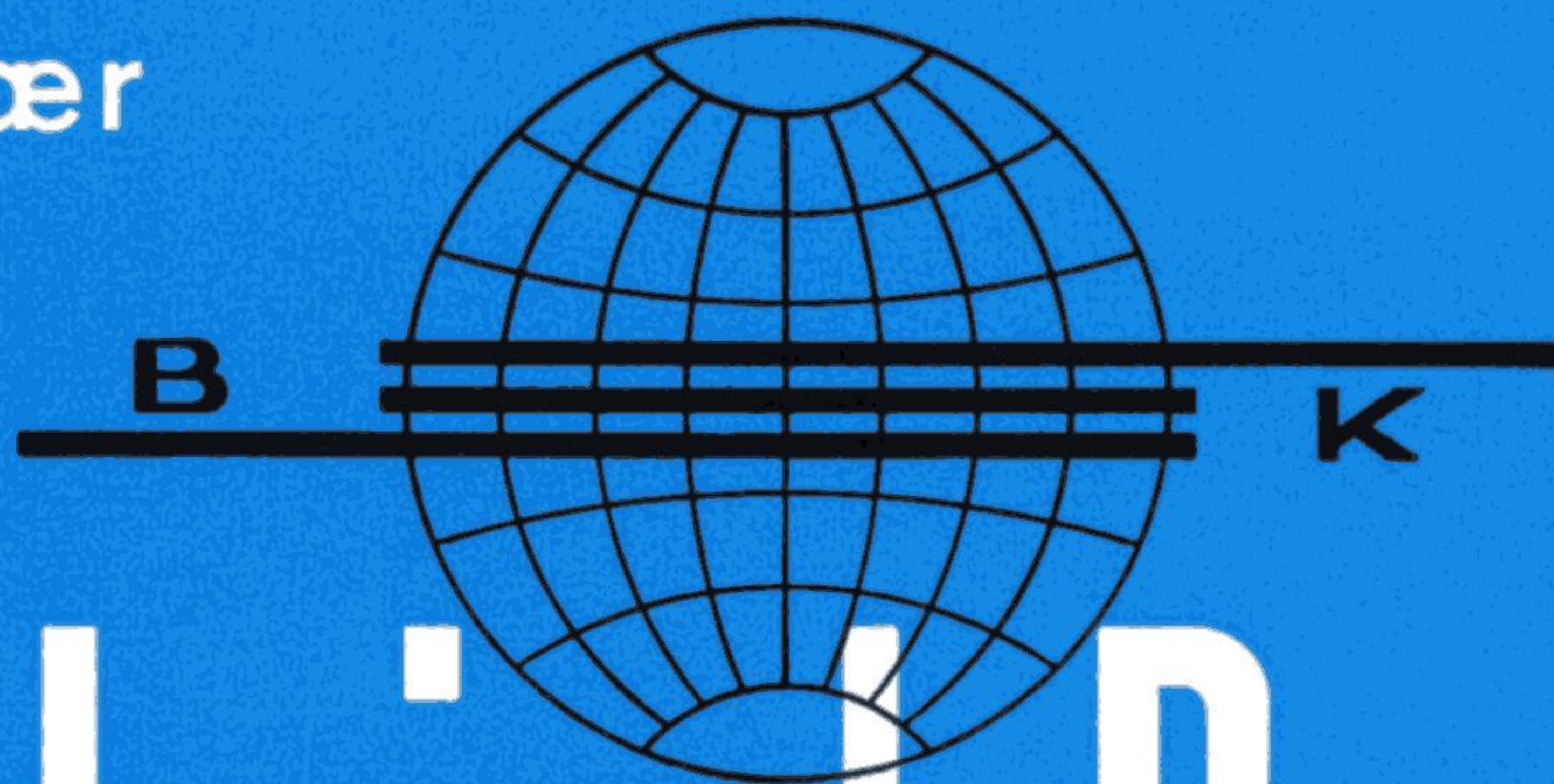
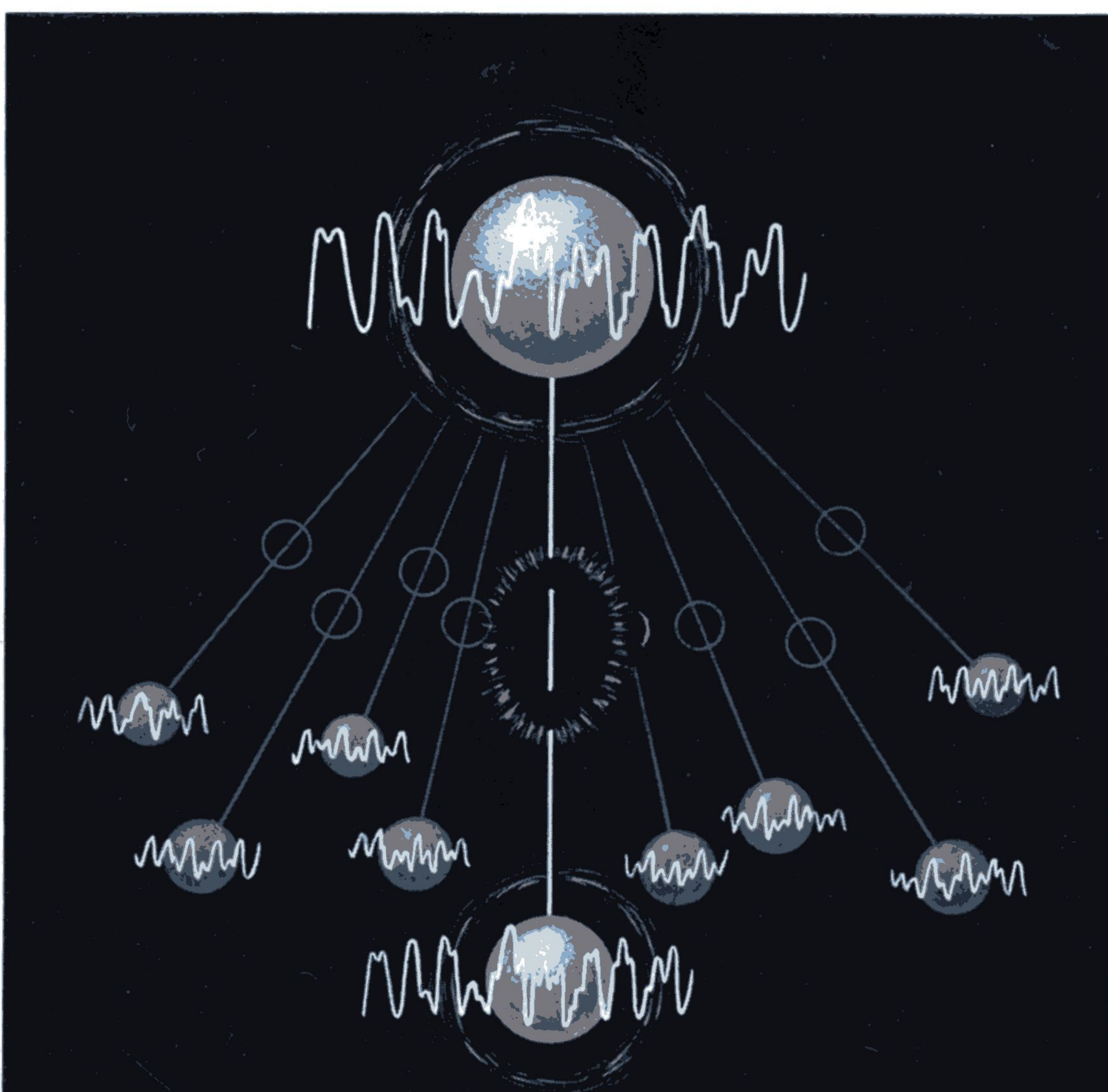


Brüel & Kjær



Technical Review

To Advance Techniques in Acoustical, Electrical, and Mechanical Measurement



Measurement of
Cross-Power-Spectra

**PREVIOUSLY ISSUED NUMBERS OF
BRÜEL & KJÆR TECHNICAL REVIEW**

- 1-1964 Statistical Analysis of Sound Levels.
- 2-1964 Design and Use of a small Noise Test Chamber.
Sweep Random Vibration.
- 3-1964 Random Vibration of some Non-Linear Systems.
- 4-1964 The Accuracy of Condenser Microphone Calibration
Methods. Part I.
- 1-1965 The Accuracy of Condenser Microphone Calibration
Methods. Part II.
- 2-1965 Direct Digital Computing of Acoustical Data.
The Use of Comparison Bridges in Coil Testing.
- 3-1965 Analog Experiments Compare Improved Sweep Random
Tests with Wide Band Random and Sweep Sine Tests
The Frequency Response Tracer Type 4709.
- 4-1965 Aircraft Noise Measurement, Evaluation and Control.
- 1-1966 Windscreening of Outdoor Microphones.
A New Artificial Mouth.
- 2-1966 Some Experimental Tests with Sweep Random Vibration
- 3-1966 Measurement and Description of Shock.
- 4-1966 Measurement of Reverberation.
- 1-1967 FM Tape Recording.
Vibration Measurements at the Technical University of
Denmark.
- 2-1967 Mechanical Failure Forecast by Vibration Analysis.
Tapping Machines for Measuring Impact Sound
Transmission.
- 3-1967 Vibration Testing – The Reasons and the Means.
- 4-1967 Changing the Noise Spectrum of Pulse Jet Engines.
On the Averaging Time of Level Recorders.
- 1-1968 Peak Distribution Effects in Random Load Fatigue.
- 2-1968 The Anechoic Chambers at the Technical University
of Denmark.

TECHNICAL REVIEW

No. 3 - 1968

Contents

	Page
On the Measurement and Interpretation of Cross-Power-Spectra By J. Trampe Broch, Dipl. Ing. E.T.H.	3
Cross Power Spectral Density Measurements with Brüel & Kjær Instruments (Part 1) By Pavel Urban and Vladimir Kop	21
News from the Factory	32

On the Measurement and Interpretation of Cross-Power-Spectra*)

by

Jens Trampe Broch, Dipl. Ing. E.T.H.
A/S Brüel & Kjær, Denmark

ABSTRACT

The mathematical correlation function technique has been utilized for a long time in turbulence research and other studies of randomly fluctuating phenomena. It has, however, been difficult to obtain the dependable analog time delay units required for a complete experimental investigation of the correlation function. By determining the so-called *cross-power spectral density function*, which is the Fourier transform of the correlation function, the use of time delay units can be avoided, and the correlation can be measured directly as a function of frequency. This paper outlines the basic theory of the cross-power spectrum technique and discusses some aspects of practical measurements. A relationship between the bandwidth of the filters used in the measuring system and the time difference between the two signals which are to be correlated is given. It is shown that for cross-spectral density measurements to be correct to within some 5 % the requirement

$$\Delta f \tau \leq 0,2$$

must be fulfilled. Here Δf is the filter bandwidth used for the analysis and τ is the time difference between the two signals.

Finally, it is shown how the cross-power spectrum technique can be used to determine complex transfer characteristics of physical systems without interfering with the systems' normal operation, to determine time delays in acoustic wave fields and to estimate the dependency of correlation coefficients upon frequency.

SOMMAIRE

La technique de la fonction mathématique de corrélation est utilisée depuis longtemps dans l'étude des turbulences et d'autres phénomènes variant de façon aléatoire.

Il a cependant été très difficile d'obtenir les retardateurs analogique fiables requis pour les recherches expérimentales complètes de la fonction de corrélation.

En déterminant la fonction de densité interspectrale, ainsi appelée, que est la transformée de Fourier de la fonction de corrélation, l'utilisation d'unités à retard peut être évitée et la corrélation peut être mesurée directement comme une fonction de la fréquence. Cet article esquisse la théorie de base de la technique de mesure interspectrale et donne quelques aspects pratiques. Un rapport entre la largeur de bande des filtres utilisés dans le système de mesure et la différence de temps entre les deux signaux à mettre en corrélation est donné. Il apparait que, pour que les mesures de densité interspectrale soient correctes à quelques 5 % pres, la condition requise

$$\Delta f \tau \leq 0,2$$

doit être remplie. Ici Δf est la largeur de bande du filtre utilisée pour l'analyse et τ est la différence de temps entre les deux signaux. Enfin il est démontré comment la technique de mesure interspectrale peut être utilisée pour déterminer les caractéristiques de transfert complète de systèmes physiques sans interférence dans le fonctionnement normal du système, pour déterminer les retards dans les champs d'ondes acoustiques et pour estimer la subordination à la fréquence, des coefficients de corrélation.

ZUSAMMENFASSUNG

Die Korrelationsfunktion dient seit langem als mathematisches Hilfsmittel für die Erforschung von Turbulenzen und anderen stochastisch veränderlichen Vorgängen. Es war jedoch

*) Paper presented at the 6th International Congress on Acoustics, Tokyo, Japan 21 – 28 August 1968.

schwierig, zuverlässige analoge Zeitverzögerungsglieder zu bauen, welche für eine vollständige experimentelle Ermittlung der Korrelationsfunktion benötigt werden. Durch Bestimmen der sogenannten spektralen Kreuzleistungsdichte, welche die Fourier-Transformierte der Kreuzkorrelationsfunktion darstellt, läßt sich die Verwendung von Zeitverzögerungsgliedern vermeiden, und die Korrelation kann direkt als Funktion der Frequenz gemessen werden. Nach einem Überblick über die zugrunde liegende Theorie der Kreuzleistungsspektrum-Technik werden in diesem Aufsatz einige Aspekte praktischer Messungen diskutiert. Eine Beziehung zwischen der Bandbreite Δf beider Filter in der Meßapparatur und der Zeitdifferenz τ zwischen den beiden Signalen, welche zu korrelieren sind, wird angegeben. Es zeigt sich, daß

$$\Delta f \tau \leq 0,2$$

sein muß, damit die Messungen der Kreuzleistungsdichte auf etwa 5% genau werden. Schließlich wird gezeigt, wie die Kreuzleistungsspektrum-Technik sich benutzen läßt, um komplexe Übertragungscharakteristiken physikalischer Systeme ohne Unterbrechung des normalen Betriebs zu bestimmen, um Zeitverzögerungen in Schallfeldern zu messen und um die Frequenzabhängigkeit von Korrelationskoeffizienten abzuschätzen.

Introduction

When it is desired to find the relationship, if any, between data observed at one point in a physical system and data observed at another point in the system use can be made of the methods of correlation techniques. One such method is mathematically formulated in the so-called *cross-correlation-function*:

$$\psi_{xy}(\tau) = \lim_{T \rightarrow \infty} \frac{1}{T} \int_0^T f_x(t) f_y(t + \tau) dt \quad (1)$$

where $f_x(t)$ is the magnitude of the process measured at the point x at an arbitrary instant of time, t , and $f_y(t + \tau)$ is the magnitude of the process measured at the point y at a time τ later. In general the cross-correlation function turns out to show a fairly complicated dependency of τ and to obtain meaningful data some sort of frequency analysis of the correlation relationship is necessary.

For a long time people involved in turbulence research have utilized correlation measurement techniques and analog electronic correlators, which actually were nothing but electronic multipliers without time delay circuits, have been commercially available on the market for some time. It has been, however, an expressed desire to obtain time delay units for these multipliers so that the complete correlation could be measured, both as a function of time and space. Dependable time delay units are, on the other hand, not so easy to build and very few such units have been successfully constructed according to analog principles.

There are ways out of this. One method, which is very elegant but rather expensive, is to utilize digital sampling principles. Another method, which in the authors opinion looks at least equally promising at present, is to use *analog cross-spectral-density measurements* with very narrow band frequency analyzers.

Basic Theory of the Cross Power Spectrum Technique

Mathematically the *cross-spectral-density function* is obtained by taking the Fourier transform of the cross-correlation function:

$$w_{xy}(f) = \int_{-\infty}^{\infty} \psi_{xy}(\tau) e^{-j2\pi f\tau} d\tau \quad (2)$$

where $w_{xy}(f)$ is the (complex) cross-spectral density function.

From the theory of Fourier integrals it is known that when equation (2) is valid the $\psi_{xy}(\tau)$ can also be found by inversion:

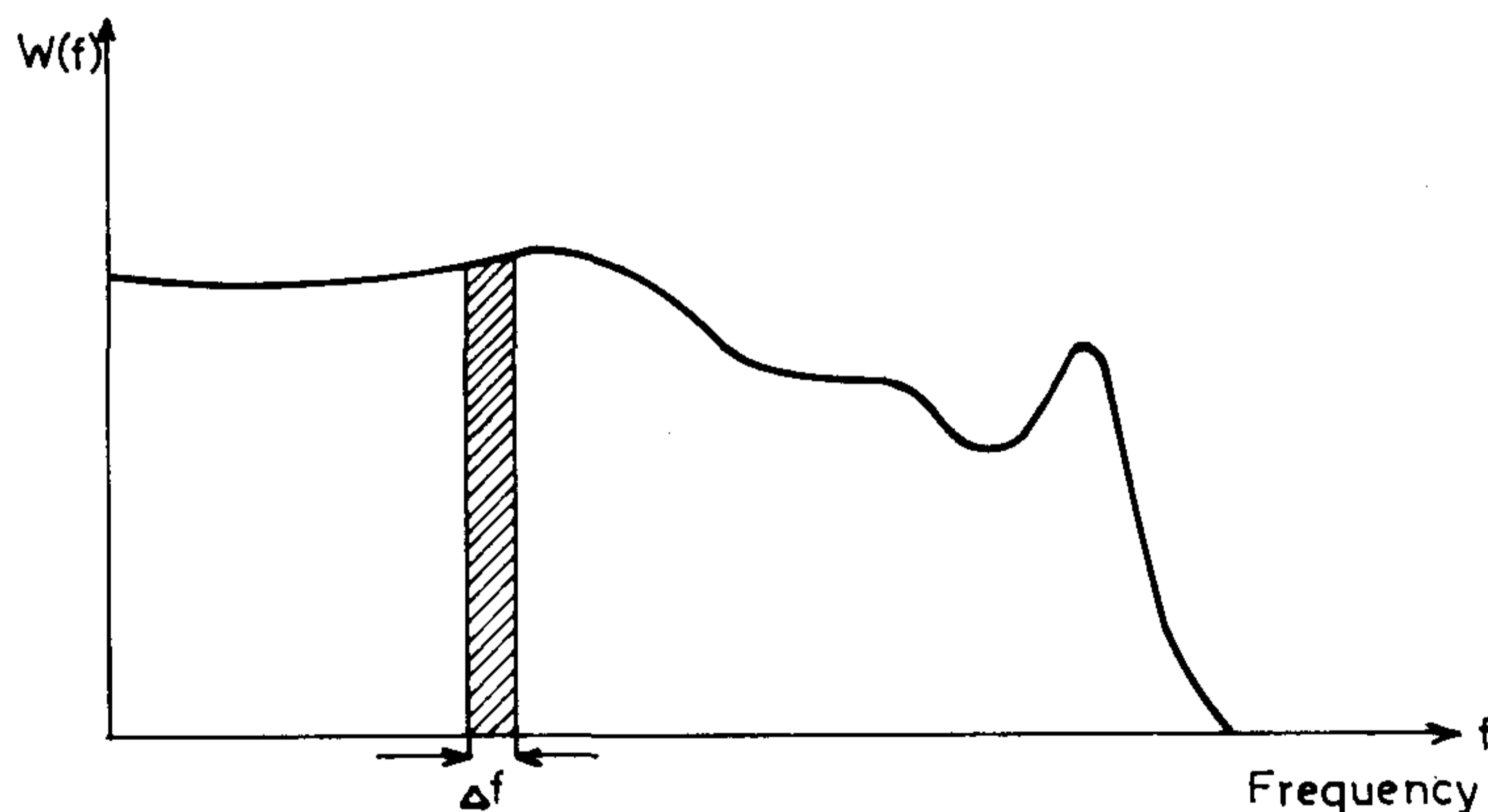
$$\psi_{xy}(\tau) = \int_{-\infty}^{\infty} w_{xy}(f) e^{j2\pi f\tau} df \quad (3)$$

writing

$$w_{xy}(f) = |w_{xy}(f)| e^{-j\varphi_f} \quad (4)$$

and considering the fact that $\psi_{xy}(\tau)$ is always a real quantity one obtains:

$$\psi_{xy}(\tau) = \int_{-\infty}^{\infty} |w_{xy}(f)| e^{j(2\pi f\tau - \varphi_f)} df = \int_{-\infty}^{\infty} |w_{xy}(f)| \cos(2\pi f\tau - \varphi_f) df \quad (5)$$



768037

Fig. 1. Illustration of an "ideal" frequency analysis.

Formula (5) can also be written:

$$\psi_{xy}(\tau) = \int_{-\infty}^{\infty} |w_{xy}(f)| \cos \varphi_f \cos(2\pi f\tau) df + \int_{-\infty}^{\infty} |w_{xy}(f)| \sin \varphi_f \sin(2\pi f\tau) df \quad (6)$$

Equations (1) and (6) form the basis for analog cross-spectral density measurements as explained below:

An ideal analog frequency analyzer will allow only that part of the signal to be measured which has frequency components within a narrow frequency band, Δf , see Fig. 1.

Assuming that no attenuation or amplification of these frequency components take place in the analyzer, and that both analyzer channels used have equal phase shifts then the cross-correlation between the two measurement channels is given by the expression:

$$(\psi_{xy})_{\Delta f} = \int_f^{f+\Delta f} 2 |w_{xy}(f)| \cos \varphi_f \cos(2\pi f\tau) df + \int_f^{f+\Delta f} 2 |w_{xy}(f)| \sin \varphi_f \sin(2\pi f\tau) df \quad (7)$$

The reason for introducing $2 |w_{xy}(f)|$ instead of $|w_{xy}(f)|$ is that in physically realizable systems only positive frequencies are involved, while $w_{xy}(f)$ was introduced for mathematical convenience where both positive and negative frequencies were considered, see equation (3).

When $\Delta f \rightarrow 0$:

$$(\psi_{xy})_{\Delta f} \approx 2 |w_{xy}(f)| \cos \varphi_f \cos(2\pi f\tau) \Delta f + 2 |w_{xy}(f)| \sin \varphi_f \sin(2\pi f\tau) \Delta f \quad (8)$$

Setting $\tau = 0$ and utilizing equations (1) and (8) one obtains:

$$2 |w_{xy}(f)| \cos \varphi_f \Delta f = \lim_{T \rightarrow \infty} \frac{1}{T} \int_0^T f_{x\Delta f}(t) f_{y\Delta f}(t) dt \quad (9)$$

Rearranging equation (9) and setting $2 |w_{xy}(f)| \cos \varphi_f = C_{xy}(f)$ gives

$$C_{xy}(f) = \lim_{\Delta f \rightarrow 0} \lim_{\Delta T \rightarrow \infty} \frac{1}{\Delta f \Delta T} \int_0^{\Delta T} f_{x\Delta p}(t) f_{y\Delta p}(t) dt \quad (10)$$

Furthermore, again utilizing equation (1) and (8), and setting $\tau = \frac{1}{4f}$

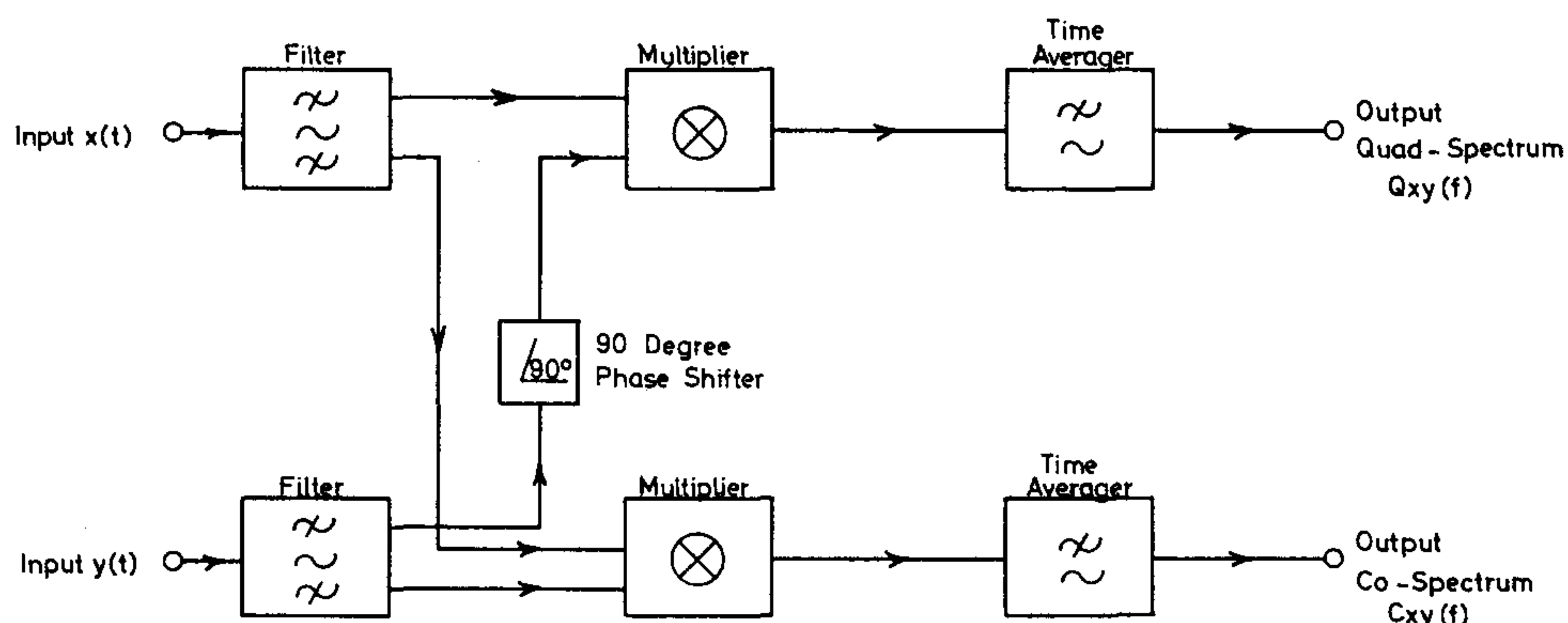


Fig. 2. Principle of operation of an analog cross-spectrum analyzer.

(90° phase shift) gives:

$$Q_{xy}(f) = \lim_{\Delta f \rightarrow 0} \lim_{T \rightarrow \infty} \frac{1}{\Delta f T} \int_0^T f_{x\Delta f}(t) f_{y\Delta f}^*(t) dt \quad (11)$$

where $Q_{xy}(f) = 2 |w_{xy}(f)| \sin \varphi_f$ and $f_{y\Delta f}^*$ is equal to $f_{y\Delta f}$ shifted 90° in phase. $C_{xy}(f)$ is denoted as the *co-spectral density function* while $Q_{xy}(f)$ is the *quadrature (quad) spectral density function*.

Fig. 2 shows the principle of analog cross-spectral density measurements and it is seen that the main operations necessary are filtering, the shifting in phase of one of the filtered signals by 90° and a multiplication of the two signals. The shifting in phase is possible in the new Brüel & Kjær *Heterodyne*

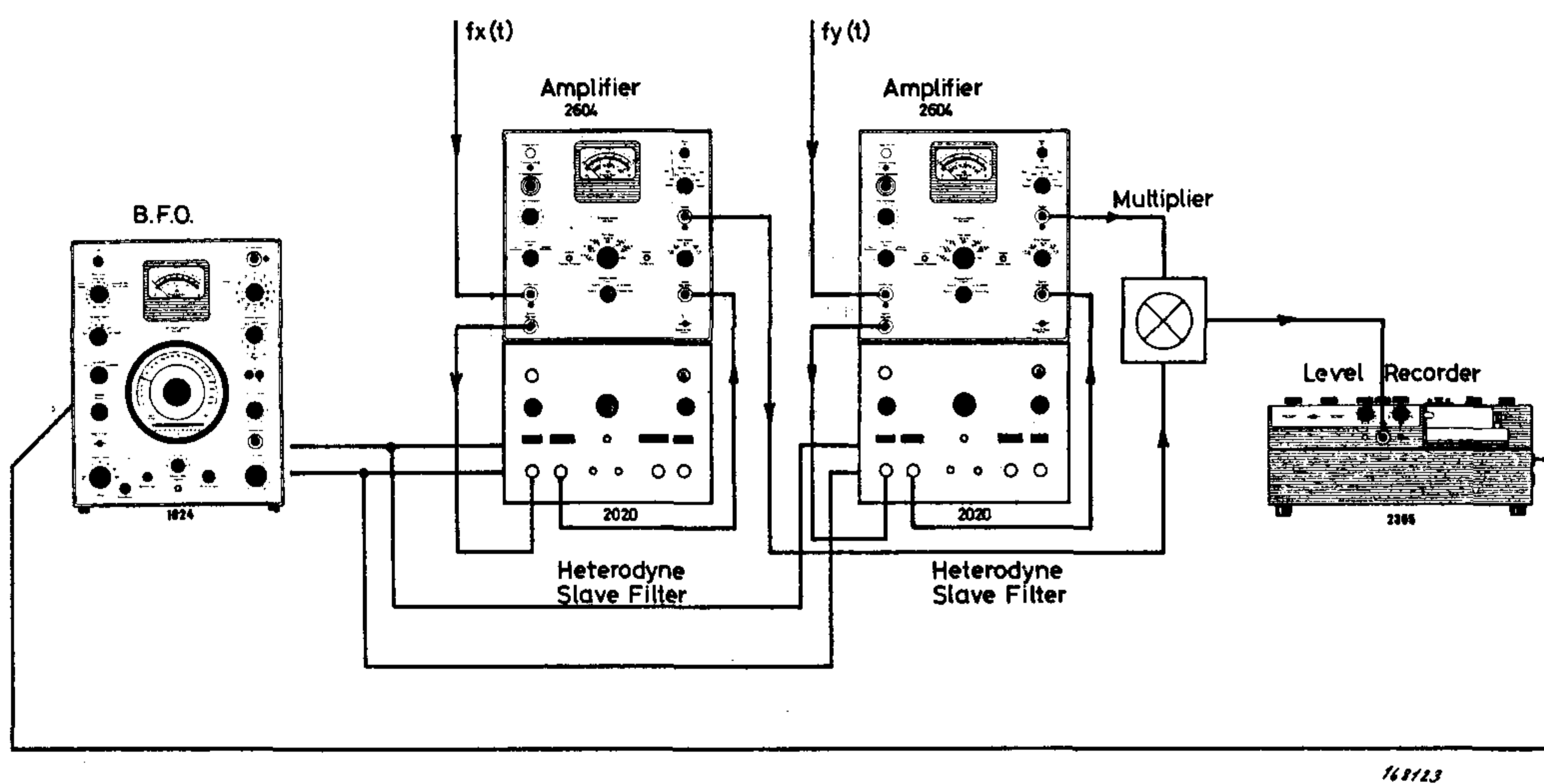


Fig. 3. Practical measuring set up for cross-spectrum analysis utilizing two Heterodyne Slave Filters Type 2020.

Slave Filter Type 2020 which has been designed with a view to also allow for cross-spectral density measurements. A typical measuring arrangement utilizing two Heterodyne Slave Filters is shown in Fig. 3.*)

Practical Measurement Considerations

In the practical measurement of cross-spectral density functions certain important facts have to be taken into account which may not be quite obvious from the theoretical derivations. One of the most important of these is the analyzer bandwidth/signal correlation time relationship. The mathematical Fourier transform, equation (2), actually presupposes a continuous frequency analysis with infinitely narrow band filters ($e^{-j2\pi f\tau}$). Such analog filters are

*) The multiplier used in Fig. 3 was a slightly modified Burr-Brown Model 1671/16 Function Module.

neither practical (because of the infinite analyzing time required) nor do they exist.

Commercially available analog filters have very definite bandwidths and the output of such a filter is therefore also self-correlated (auto-correlated) over very definite time intervals only. These time intervals may be regarded as the "memory" of the filter and it is clear that the multiplications required to obtain the cross spectral density function must be performed within the "memory time" of the filter. When the "memory" is not perfect the cross-spectral density function obtained will be in error. How large the error will be depends, of course, upon the "memory" of the filters and the time delay between the two signals being multiplied as demonstrated in the following.

Theoretically the autocorrelation function for the output of a box-shaped narrow band filter of bandwidth Δf can be derived by taking the Fourier transform of the output power spectrum:

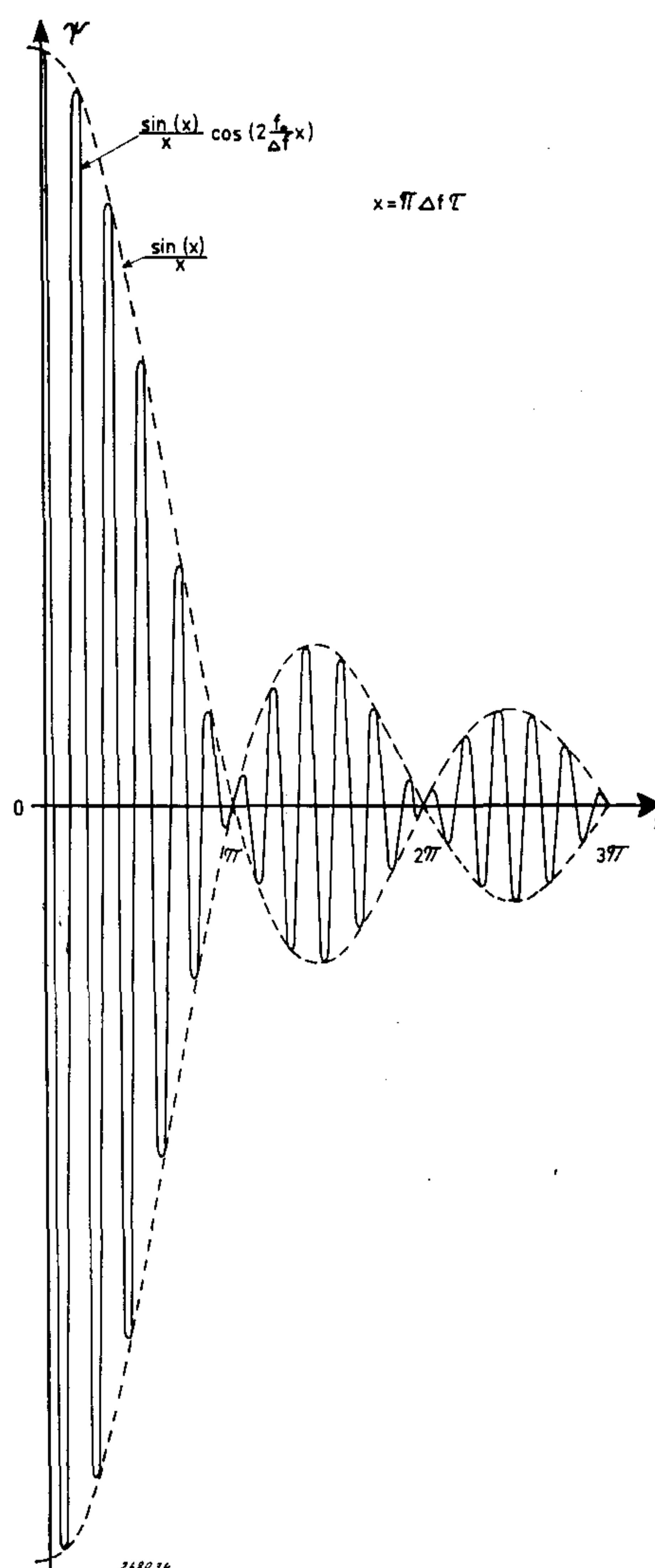


Fig. 4. Auto-correlation function for the output of a narrow band "ideal" frequency analyzer fed with Gaussian random noise.

$$\psi(\tau) = \int_{-\infty}^{\infty} w(f) e^{j2\pi f\tau} df = \int_f^{f+\Delta f} ce^{j2\pi f\tau} df \quad (12)$$

$$\psi(\tau) = c \int_f^{f+\Delta f} \cos(2\pi f\tau) df \quad (13)$$

where $c = 2w(f) = \text{constant}$.

When integrated equation (13) becomes

$$\begin{aligned} \psi(\tau) &= \frac{c}{2\pi\tau} [\sin[2\pi\tau(f+\Delta f)] - \sin(2\pi f\tau)] \\ &= \frac{c}{2\pi\tau} 2 \sin(\pi\Delta f\tau) \cos\left[2\pi\tau\left(f + \frac{\Delta f}{2}\right)\right] \end{aligned} \quad (14)$$

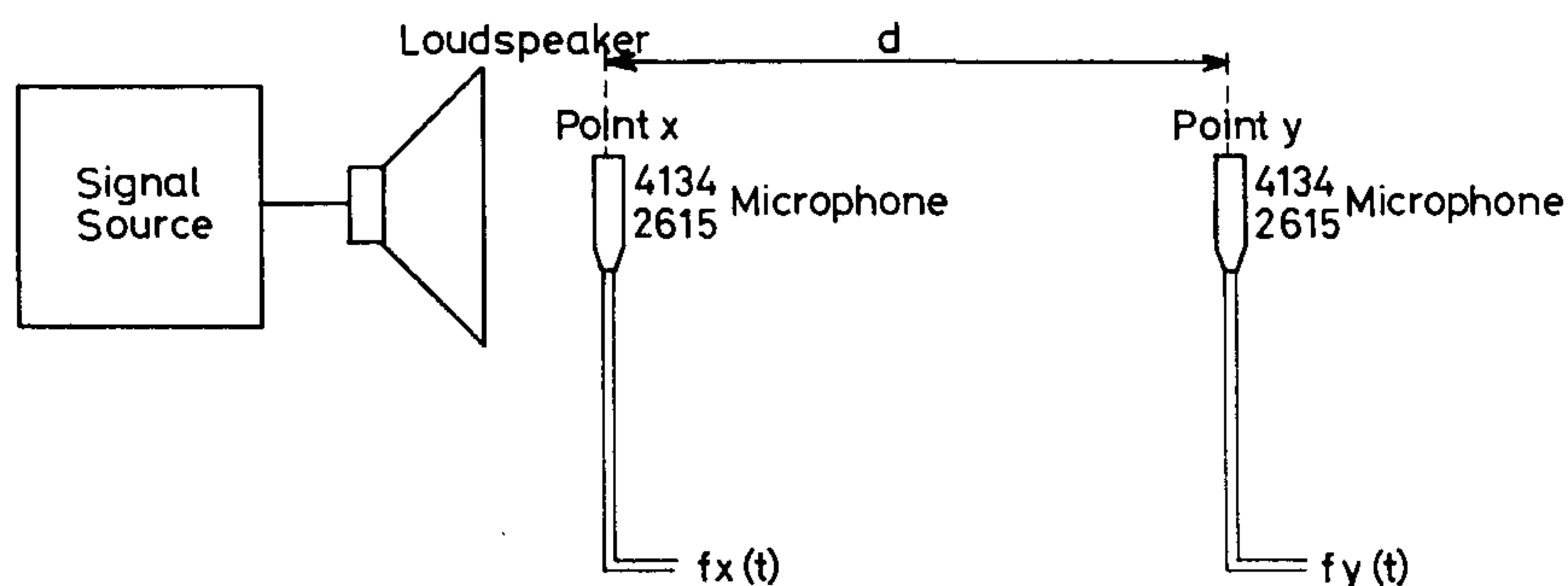
By setting $f_0 = f + \frac{\Delta f}{2}$ where f_0 here denotes the center frequency of the filter then:

$$\psi(\tau) \approx c\Delta f \frac{\sin(\pi\Delta f\tau)}{\pi\Delta f\tau} \cos(2\pi f_0\tau) \quad (15)$$

This function is plotted in Fig. 4 for the case where $c\Delta f = 1$ and $x = \pi\Delta f\tau$ and it is seen that as long as $\Delta f\tau$ is small no significant loss of "memory" will occur. The practical conclusion which can be drawn from equation (15) and Fig. 4, is that the longer the delay time τ between the inputs to the two filters used for cross-spectrum measurements is, the narrower must the bandwidth of the filters be to achieve correct results. For instance, for the cross-spectral density measurements to be correct to within some 5% the following relation is obtained from Fig. 4:

$$\Delta f\tau \leq 0.2 \quad (16)$$

In practice no filter has the exact theoretical box-shape, and some experiments have been made to investigate the influence of filter bandwidth in actual measurements. The experiments were carried out on the transmission of sound waves in an acoustically free field as illustrated in Fig. 5, and the



168124

Fig. 5. Arrangement used for measurements in an acoustic wave-field.

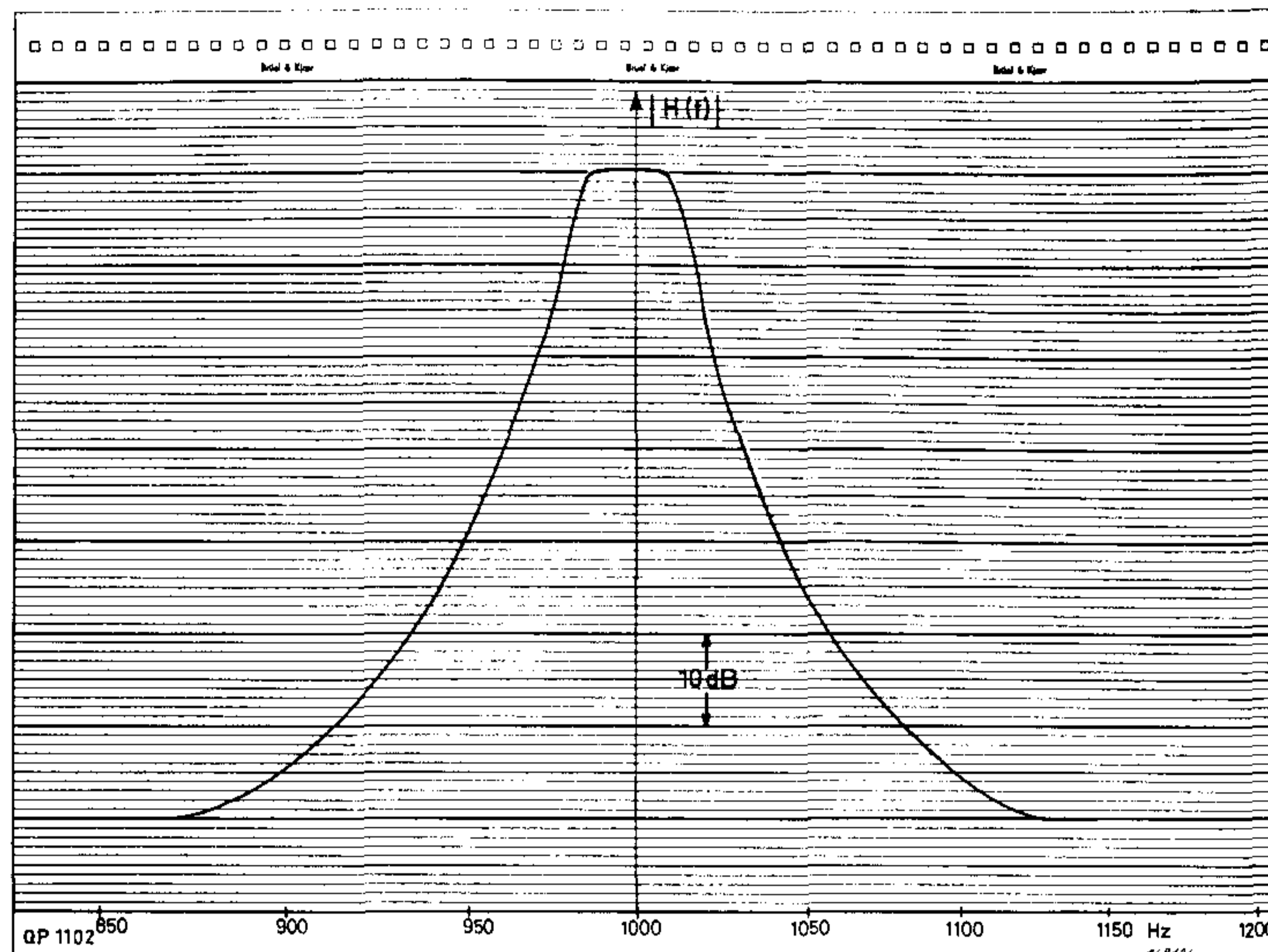


Fig. 6. Typical relative response curve for the filters used in the Heterodyne Slave Filter Type 2020.

shape of the filter curves used is shown in Fig. 6 (typical relative response curve for the Heterodyne Slave Filter Type 2020). Two different experiments were performed:

- 1) The bandwidth, Δf , of the Slave Filters were kept constant at 100 Hz and the distance, d , between the two microphones, i.e. the delay time, τ , of the sound waves, varied.
- 2) The distance between the microphone was kept constant and the bandwidth of the filters, Δf , varied.

Because the sound field was not plane, corrections for the change in sound pressure level with distance had to be applied in the first experiment. This is readily made, however, simply by measuring the sound pressure level at each microphone position used.

The results of the first experiments are given in Fig. 7 and indicate that the filters are very close to a theoretically "ideal" filter in that the measured data

fit the first lobe of the $\frac{\sin(x)}{x}$ -function almost ideally (within the measurement accuracy). This is the most important part of the correlation curve with respect to cross spectral density measurements. On the other hand, considerable deviations exist between the theoretical curve and the measured results for the second lobe of the $\frac{\sin(x)}{x}$ -function. These deviations may be due partly to the not quite "ideal" shape of the filters used, and partly to the lower accuracy of the measuring arrangement in the region of very low correlation levels. As this part of the correlation curve is of no great practical interest no further investigation of the phenomena was made.

It should be mentioned in connection with Fig. 7 that only the amplitude function $\frac{\sin(x)}{x}$ of equation (15) has been utilized for comparison between

theory and practical measurements. In equation (15) also an oscillating part, $\cos(2\pi f_0 \tau)$, is included, which means that for more or less arbitrary values of f_0 and τ one may not actually measure the maximum amplitude value determined by the $\frac{\sin(x)}{x}$ -function, see also Fig. 4. To "exclude" the oscillating part of equation (15), however, it is only necessary to measure both the functions $\frac{\sin(x)}{x} \cos(2\pi f_0 \tau)$ and $\frac{\sin(x)}{x} \sin(2\pi f_0 \tau)$

to square the two values so obtained, add them and take the square – root of the sum:

$$\sqrt{\left[\frac{\sin(x)}{x}\right]^2 \cos^2(2\pi f_0 \tau) + \left[\frac{\sin(x)}{x}\right]^2 \sin^2(2\pi f_0 \tau)} = \frac{\sin(x)}{x}$$

Because the value of $\frac{\sin(x)}{x} \sin(2\pi f_0 \tau)$ is equal to $\frac{\sin(x)}{x} \cos(2\pi f_0 \tau)$ shifted

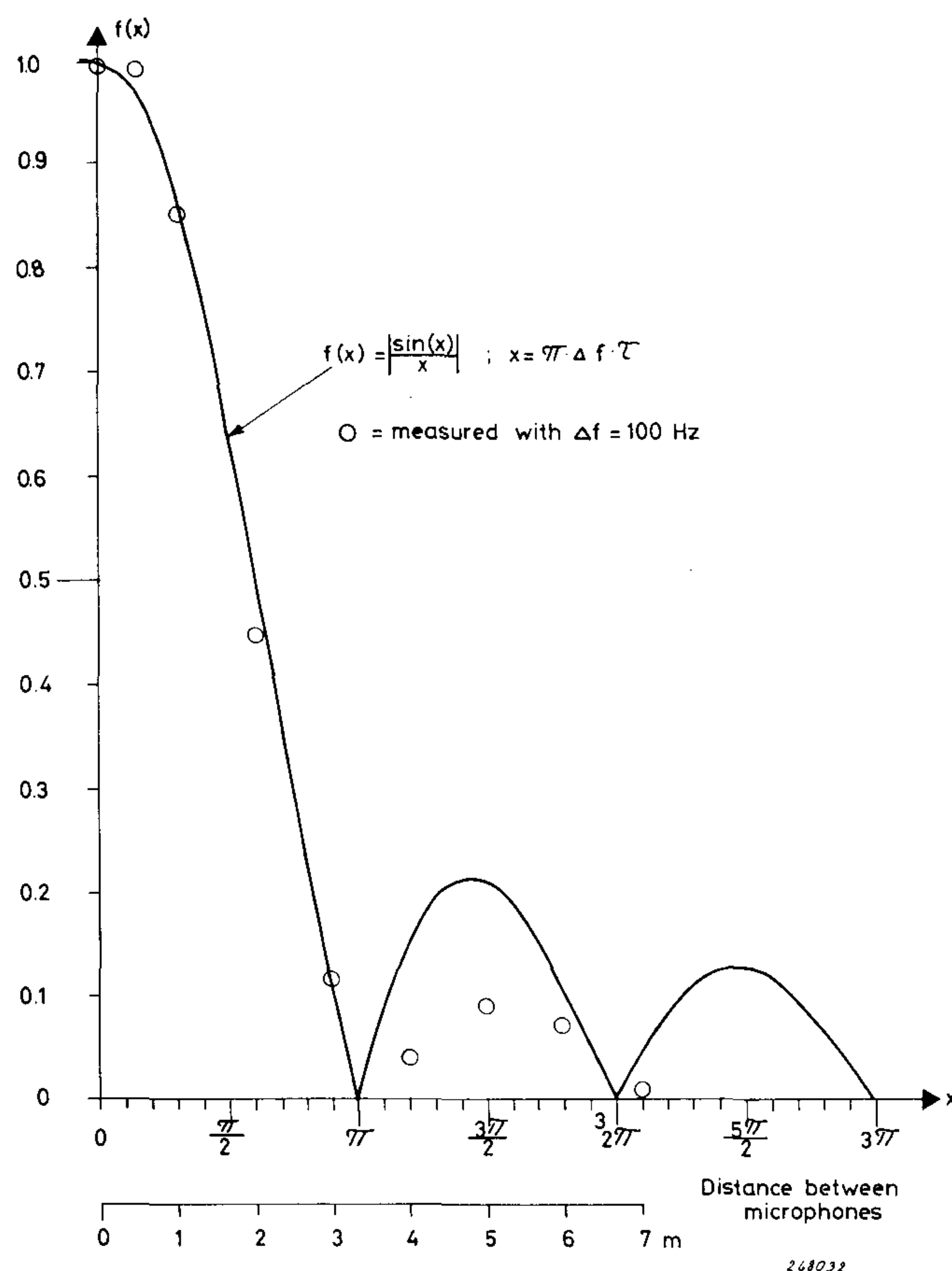
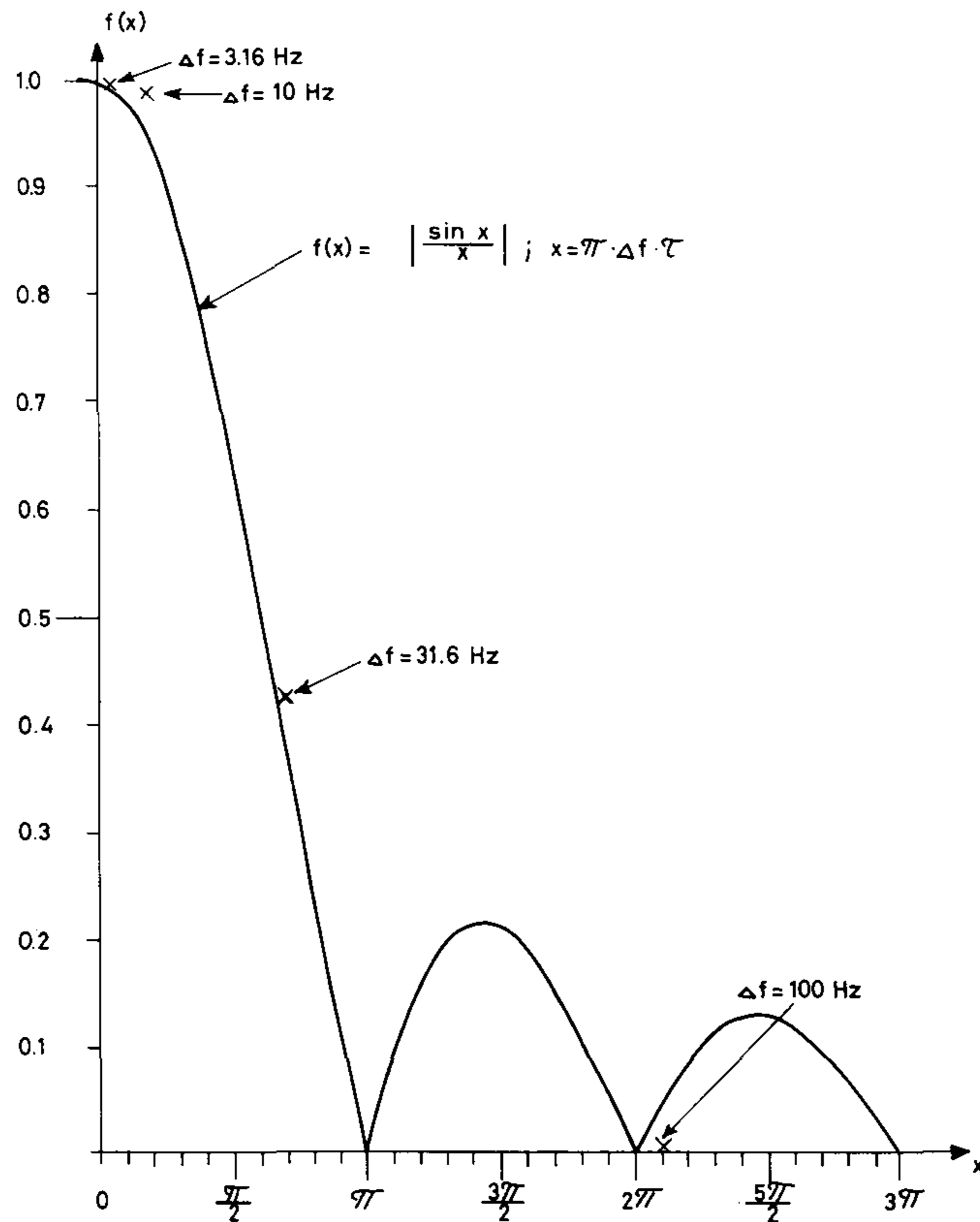


Fig. 7. Comparison between the theoretical $\frac{\sin(x)}{x}$ -function and results obtained from measurements with the Heterodyne Slave Filter.

90° in phase it can be readily found by utilizing the 90° phase shift arrangement included in the Heterodyne Slave Filter. The above described technique was used to obtain the data shown in Fig. 7.

Fig. 8 shows the results from the second experiments. Here the distance between the two microphones was kept constant and the filter bandwidth



248033

Fig. 8. Effect of the variation in filter bandwidth upon the measured cross power spectral density when the delay time between the signals $f_x(t)$ and $f_y(t)$ was of the order of 20 msec.

varied: $\Delta f = 3.16$ Hz, $\Delta f = 10$ Hz, $\Delta f = 31.6$ Hz and $\Delta f = 100$ Hz. The distance between the microphones was approximately 7 meters and it can be seen that excellent correlation was obtained both in the case of the 3.16 Hz bandwidth and in the case of the 10 Hz bandwidth. This was also to be expected from theoretical considerations. When the filter bandwidth was changed to 31.6 Hz the correlation level was reduced to 0.42 and for a filter bandwidth of 100 Hz practically no correlation could be measured (see also Fig. 7: $\Delta f = 100$ Hz, $d = 7$ m).

From the experimental results it may be concluded that the theoretical relationships given in equations (15) and (16) also hold true for the Heterodyne Slave Filter Type 2020.

In addition to the analyzer bandwidth/signal correlation time error discussed above and formulated f. inst. in equation (16) another type of error has to be taken into account when cross spectral density measurements are made on random signals. This is the "normal" statistical error:

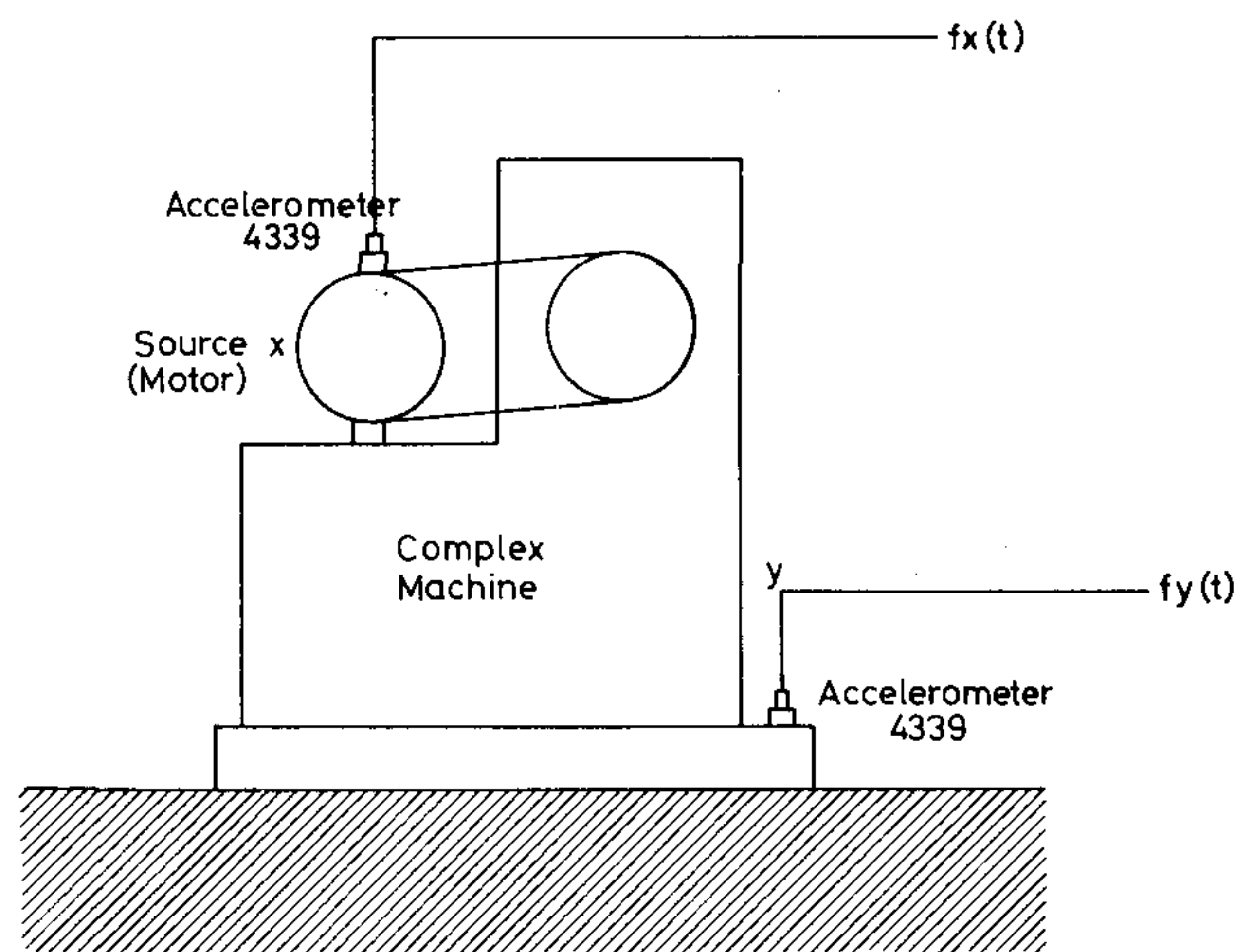
$$\boxed{\varepsilon = \frac{1}{\sqrt{\Delta f T}}} \quad (17)$$

where T is the averaging time used in the multiplication (see equations (10) and (11)).

An interesting conclusion which can be drawn from equation (17) in conjunction with the analyzer bandwidth/signal correlation time requirement is that for a given averaging time, T , a decrease in filter bandwidth decreases the correlation time error but increases the statistical error, i.e. the two requirements are in this case conflicting. If, for some reason, the averaging time in a particular measurement cannot be increased the analyzer bandwidth must therefore be chosen to compromise between the two types of error, a fact which may be worth while remembering when cross spectral density measurements are to be made.

Applications of the Cross Power Spectrum Technique

One of the most interesting applications of the cross power spectrum technique is its ability to determine the complex transfer characteristic from the source to any point in a physical system. This may be of special interest in the study of shipboard, aircraft or space-vehicle vibrations, but has also been used in vibration studies on automobiles and special machinery. The relation between the cross power spectral density measured between the source x and the



768125

Fig. 9. Illustration of transfer characteristic measurements on a complex machine without interfering with the machine's normal operation.

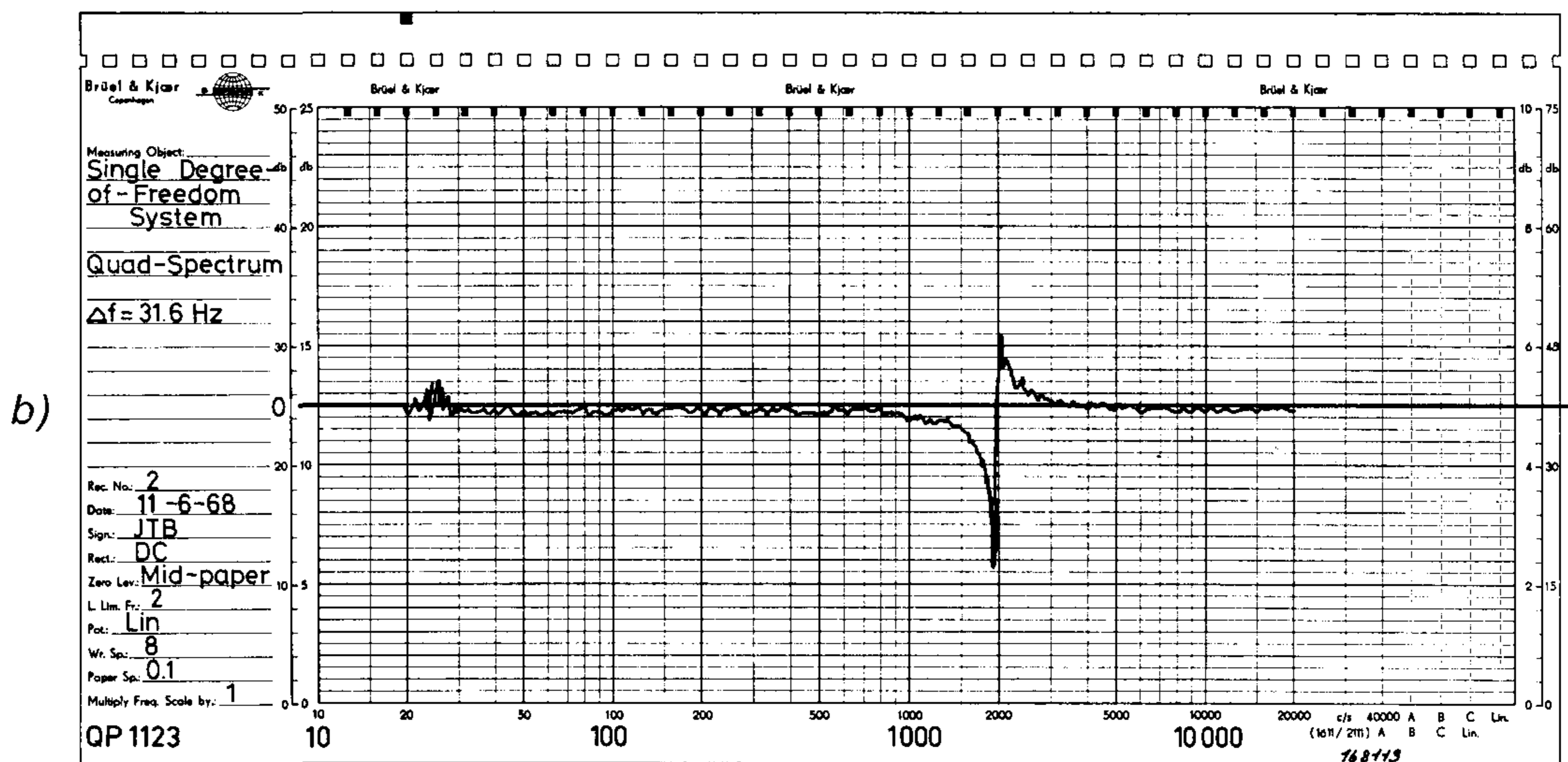
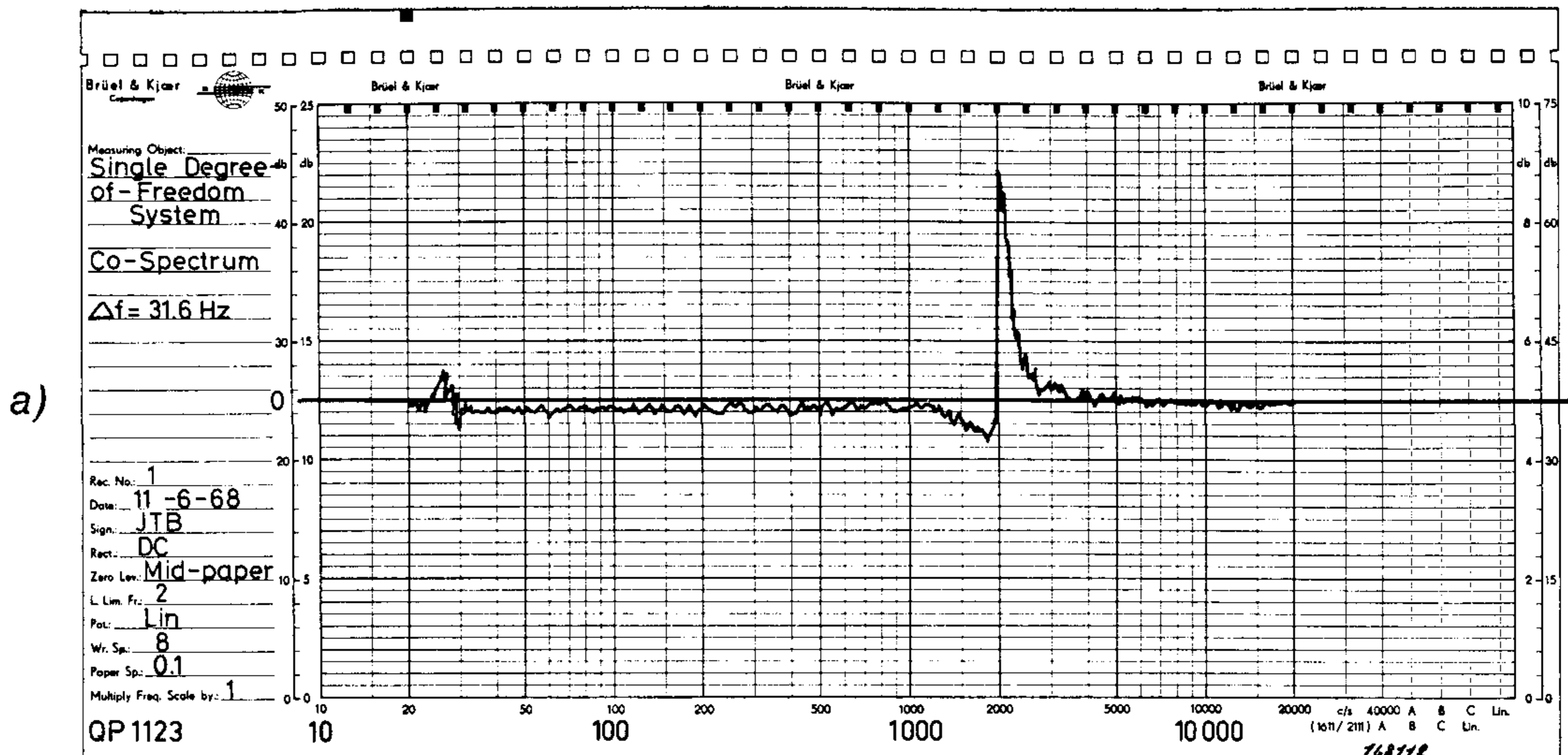


Fig. 10. Cross spectral density curves relating the output to the input of a simple single degree-of-freedom system excited by "white" random noise.
 a) Co-spectral density curve.
 b) Quad spectral density curve.

point y in the system, Fig. 9, the ordinary power spectral density measured at x , and the (complex) transfer characteristic between x and y is:

$$w_{xy}(f) = H_{xy}(f) w_{xx}(f) \quad (18)$$

Here: $w_{xy}(f)$ = Cross power spectral density

$H_{xy}(f) = |H_{xy}(f)| e^{-j\varphi_{xy}(f)}$ = Complex transfer characteristic between x and y .

$w_{xx}(f)$ = Power spectral density at x

It should be pointed out at this stage that

$$|w_{xy}(f)| = \sqrt{C_{xy}(f)^2 + Q_{yx}(f)^2} \quad (19)$$

and

$$\varphi_{xy}(f) = \tan^{-1} \left(\frac{Q_{xy}(f)}{C_{xy}(f)} \right) \quad (20)$$

see also equations (4), (10) and (11) on p. 3 and 4.

Thus from the measurement of the co- and quad spectral density functions between the points x and y as well as the power spectral density function at x it is a relatively easy matter to determine $H_{xy}(f)$ both with respect to magnitude and with respect to phase at each frequency band of interest.

To demonstrate the use of this technique two simple measurements have been made at Brüel & Kjær on analog models.

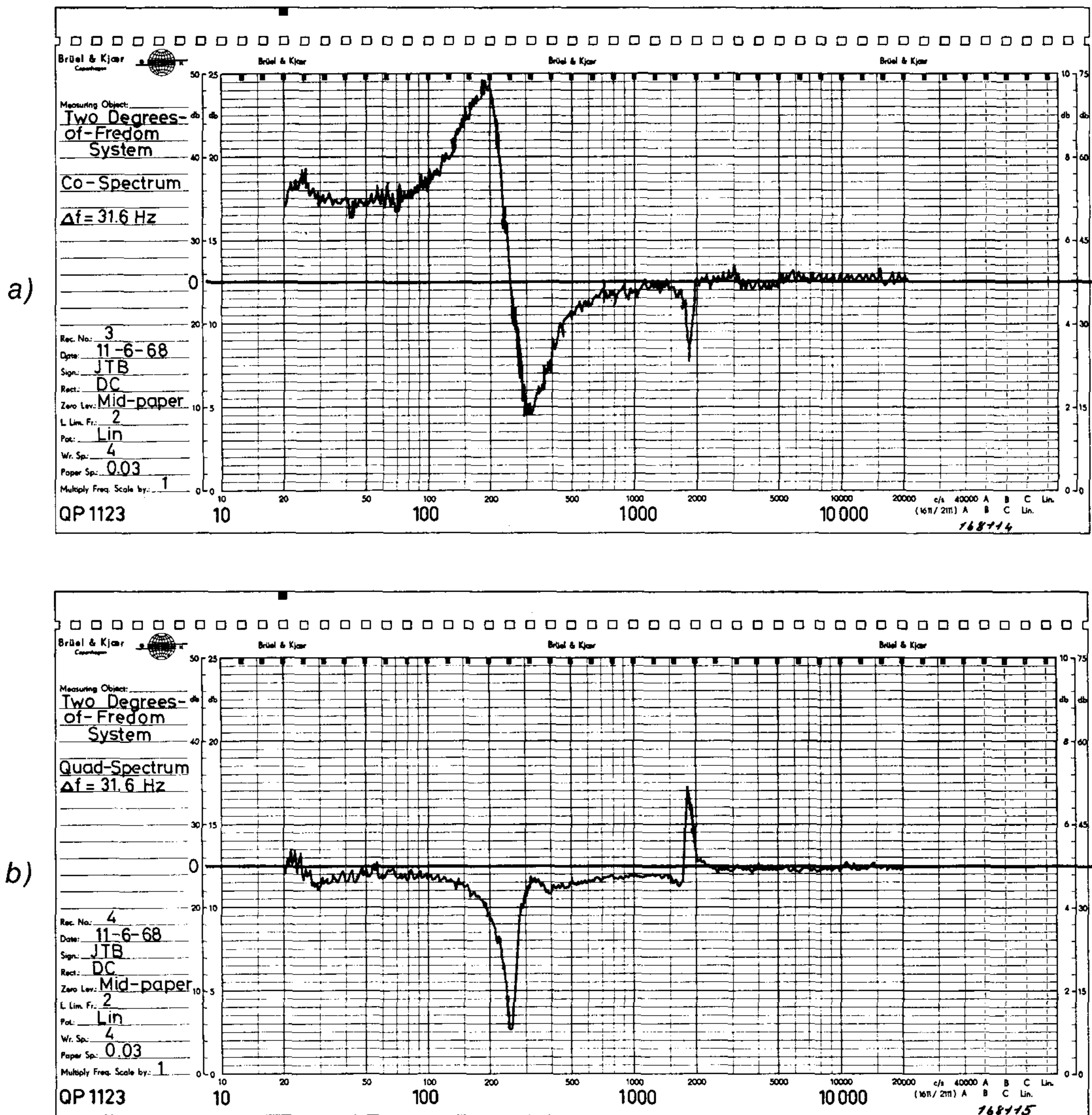


Fig. 11. Similar to Fig. 10 except that in this case the system being investigated was a two degrees-of-freedom system.
 a) Co-spectral density curve.
 b) Quad spectral density curve.

The results of the first experiment are shown in Fig. 10, and was obtained from measurements on a single degree-of-freedom system excited by white random noise. (The same results could in this simple case have been obtained by exciting the system with a sweeping sine wave signal of constant RMS level). To allow for correct recording of both positive and negative values of the co- and quad spectrum the Level Recorder was supplied with a linear range potentiometer biased to deflect to the center line of the recording paper for zero output from the multiplier.

Similarly Fig. 11 shows the results of measurements on a more complicated system (a two degrees-of-freedom system).

Because the recordings are made automatically on frequency calibrated paper the co- and quad spectrum component can be read directly off the recording at any particular frequency and the computations according to equations (19) and (20) be readily performed.

Another interesting application of the technique discussed in this paper is *the possibilities it offers for the measurement of effective time delays in acoustical or mechanical wave fields*. This may be best demonstrated by measurements in an acoustically free field, such as the sound field produced by a loudspeaker placed in a large anechoic chamber. The measurement arrangement used for these experiments was the same as that shown in Fig. 5, p. 7.

As measurements on random signals using very narrow band filters are very time consuming the measurements were this time made by means of a sweeping sine wave signal. Two different distances were used between the measuring microphones.

The results of the measurements are shown in Figs. 12 and 13 and demonstrate clearly the wave phase-effect.

To derive a simple formula which allows the calculation of time delays from the spectra shown in Figs. 12 and 13 consider the following:

If the signal at the point x is $A \sin(2\pi ft)$ and represent a free progressive wave then the signal at the point y will be $B \sin(2\pi ft + \varphi_t)$ where

$$\varphi_t = \frac{d}{\lambda} 2\pi \quad (21)$$

d = Distance between the points x and y .

λ = Wavelength of the sound wave of frequency f .

As $\lambda = \frac{v}{f}$ where v is the velocity of sound then

$$\varphi_t = 2\pi \frac{fd}{v} = 2\pi\tau_t f \quad (22)$$

Here $\tau_t = \frac{d}{v}$ = transmission time of the wave from the point x to the point y .

The co-spectrum of the signals at x and y is:

$$C_{xy} = \lim_{T \rightarrow \infty} \frac{1}{T} \int_0^T AB \sin(2\pi ft) \sin(2\pi ft + \varphi_f) dt =$$

$$= \frac{1}{2} AB \cos \varphi_f \quad (23)$$

which will vary with frequency as $\cos \varphi_f$. Now $\cos \varphi_f = 0$ when $\varphi_f = n \frac{\pi}{2}$ whereby the following conditions for zero crossings of the co-spectrum can be obtained from equation (22):

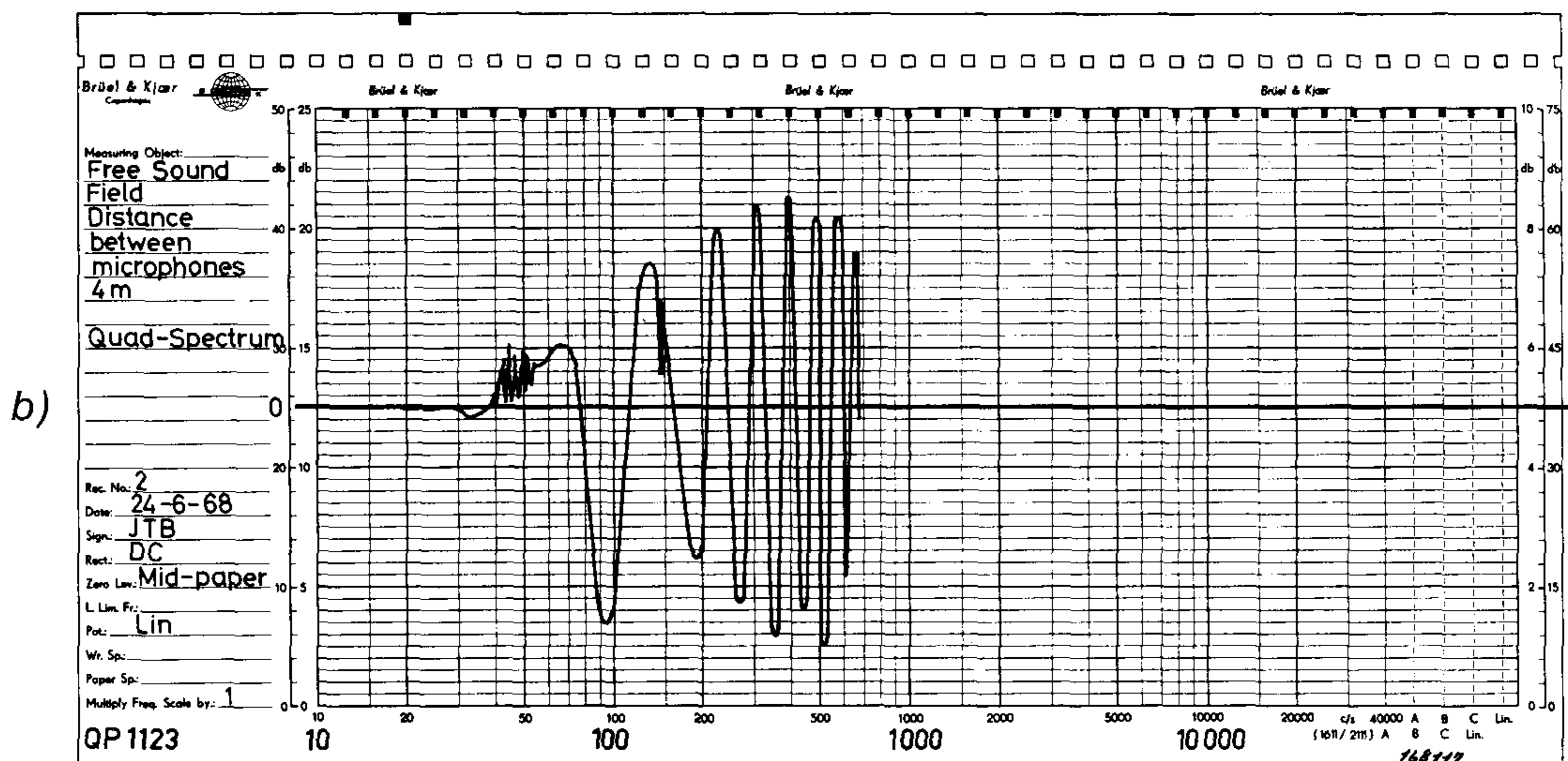
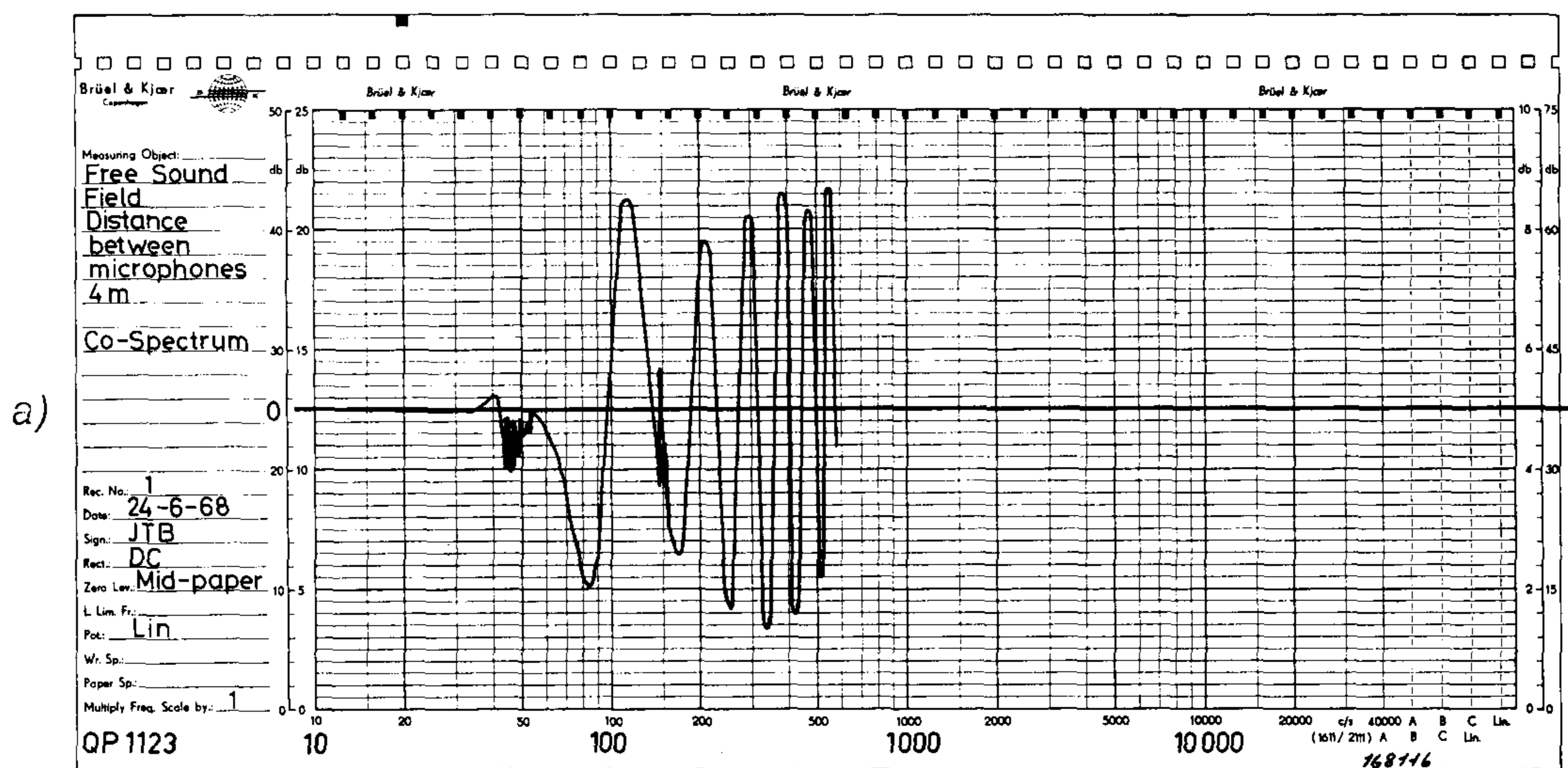


Fig. 12. Results obtained from measurements in an acoustically free field.
Distance between microphones 4 m.
a) Co-spectral density curve.
b) Quad spectral density curve.

$$2 \pi \tau_i f_n = n \frac{\pi}{2} \quad \text{and} \quad 2 \pi \tau_i f_{n-1} = (n-1) \frac{\pi}{2} \quad (24)$$

By subtracting the two equations (24) the following simple relationship is obtained between the transmission time τ_i of the wave, the distance, d , between the measurement points and two successive zero-crossing of the co-spectrum:

$$\tau_i = \frac{d}{v} = \frac{1}{2(f_n - f_{n-1})} \quad (25)$$

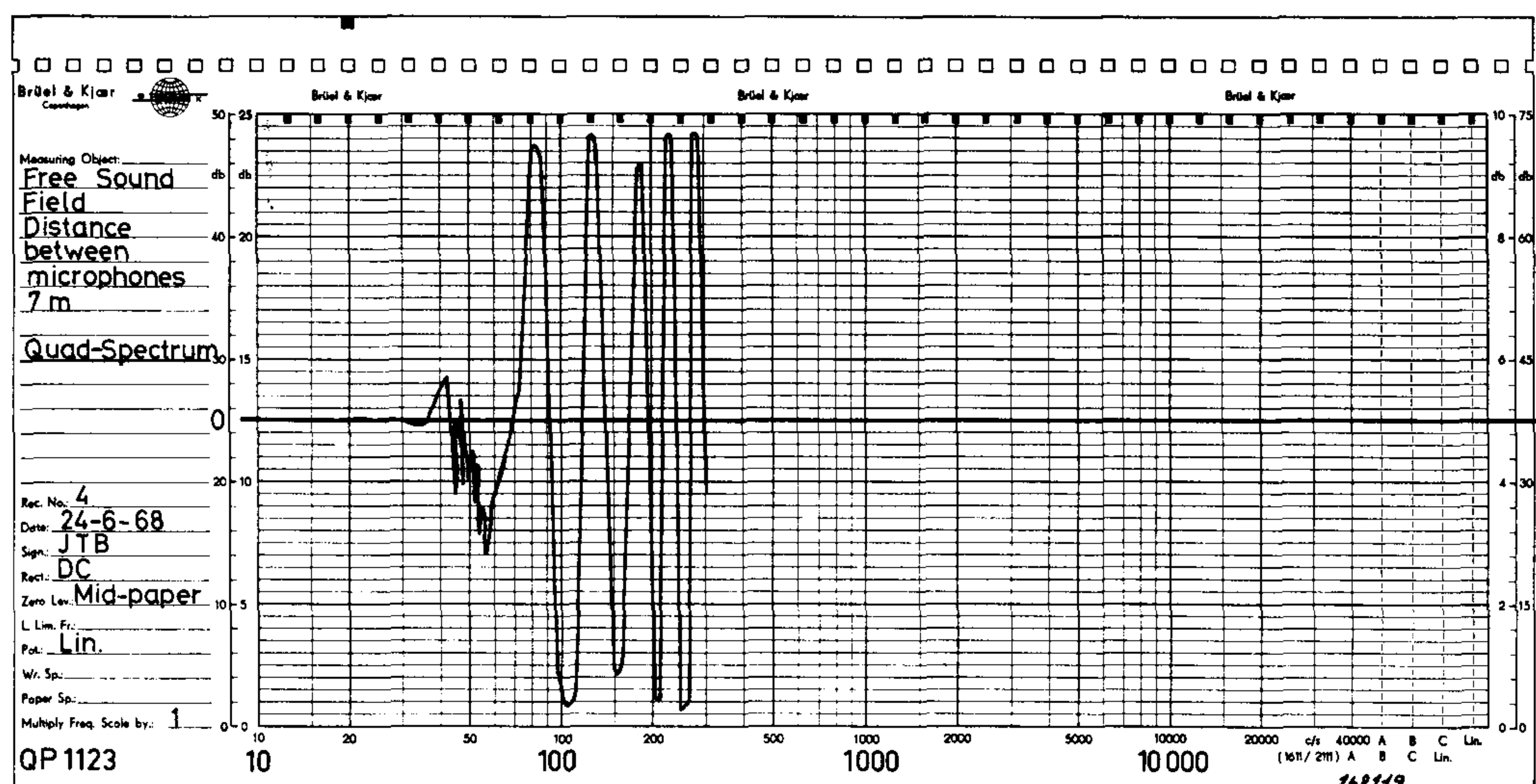
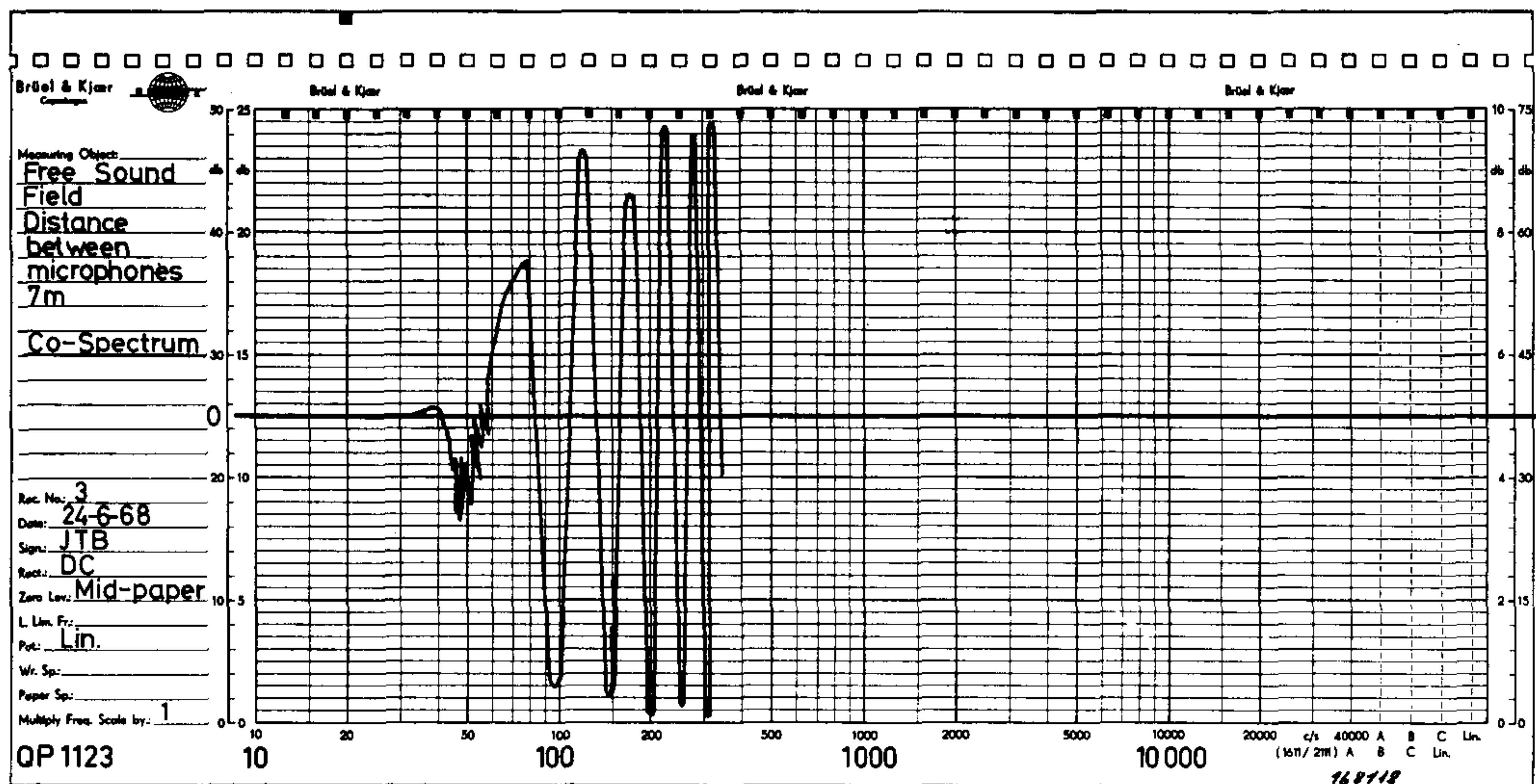


Fig. 13. Similar to Fig. 12. Distance between microphones 7 m.
 a) Co-spectral density curve.
 b) Quad spectral density curve.

The same relationship is, of course, obtained for zero-crossings of the quad spectrum with the only difference that the zero-crossings are shifted 90° in phase, see also Figs. 12 and 13.

In Figs. 12 and 13 only the first few zero-crossings are shown as the zero-crossing spectrum "blurs out" on the paper when the frequency is increased. This can be avoided by a suitable expansion of the frequency scale. It was, however, felt that for the purpose of demonstration only the first parts of the spectra were required.

By checking the distances calculated from equation (25) with the actually measured distances between the microphones extremely good correlation was found.

Finally, it should be pointed out that by measuring *both* the cross spectral density between the signals observed at the points x and y in a physical system *and* the ordinary power spectral density at both points *the correlation coefficient* R_{xy} , between the two signals can be calculated from the formula:

$$R_{xy} = \sqrt{\frac{|W_{xy}|^2}{W_{xx} W_{yy}}} \quad (26)$$

As this coefficient depends on *frequency* it is normally termed *coherence function* (to distinguish it from the correlation function which is defined in the time domain). The coherence function is often denoted by $\gamma_{xy}(f)$ whereby equation (26) takes the form:

$$\gamma_{xy}(f) = \sqrt{\frac{|W_{xy}(f)|^2}{W_{xx}(f) W_{yy}(f)}} \quad (27)$$

Conclusion

The practical cross power spectrum technique, as discussed in the preceding text, has received relatively little attention to date. Although the basic theory has been available for some time its actual practical value seems to have been underestimated and very little instrumentation suited for cross spectral density measurements has been commercially available. In the author's opinion the cross power spectrum technique represents a very powerful tool in cases where ordinary transfer function measurements are difficult to make.

Apart from *complete transfer characteristic determinations* the cross power spectrum, as demonstrated, also allows *correlation coefficients and time delays to be determined directly as a function of frequency* without the use of vast mathematical machinery.

Furthermore, as the measurements can often be made *without interfering with the system's normal operation* this "new" technique is deemed to become a significant factor in tomorrow's measurement technology.

Bibliography:

BENDAT, J. S. and
PIERSOL, A. G.:

Measurement and Analysis of Random Data.
John Wiley & Sons Inc. New York 1966.

CLARKSON, B. L. and
MERCER, C. A.:

Note on the Use of Cross Correlation in Studying
the Response of Lightly Damped Structures to Noise.
ISAV Memorandum No. 116, Nov. 1964. University of
Southampton. U.K.

Cross Power Spectral Density Measurements with Brüel & Kjær Instruments. (Part 1).

By

Pavel Urban and Vladimir Kop,
Motor Car Research Institute, Prague.

ABSTRACT

After a discussion of some aspects of the cross-power spectrum theory it is shown how two B & K Audio Frequency Spectrometers Type 2112 may be utilized to determine the cross-power spectrum of electrical and mechanical phenomena. To obtain the phase shift required to measure the quad-spectrum two so-called Gorges bridges were used. The principle of operation and basic circuit diagram for the bridges are outlined, and some practical cross spectrum measurements briefly described.

SOMMAIRE

Après un exposé de quelques aspects de la théorie interspectrale, on montre comment deux spectromètres B.F. Brüel & Kjær type 2112 peuvent être utilisés pour déterminer l'interspectre de puissance de phénomènes électriques et mécaniques. Pour obtenir le décalage de phase requis pour mesurer le spectre de la composante en quadrature, deux ponts de Gorges sont employés. Le principe de fonctionnement et le schéma de principe des ponts sont décrits et quelques mesures pratiques interspectrales sont brièvement exposées.

ZUSAMMENFASSUNG

Zunächst werden einige Aspekte der Kreuzleistungsspektrum-Theorie erörtert; dann wird gezeigt, wie sich zwei B & K-Terz/Oktav-Analysatoren Typ 2112 dazu verwenden lassen, das Kreuzleistungsspektrum elektrischer und mechanischer Phänomene zu bestimmen. Um die zum Messen des Quad-Spektrums (Imaginärteil) erforderliche Phasendrehung zu bewirken, wurden zwei sogenannte Gorges-Brücken benutzt. Das Arbeitsprinzip und die Grundschaltung der Brücken werden umrissen, und einige praktische Kreuzspektrums-Messungen werden kurz beschrieben.

1. Introduction

The theoretical treatment of acoustical and mechanical phenomena has practically always been based on the use of simple harmonic signals. This simplification has until recently been quite satisfactory. Experience shows, however, that machines and plants, as met in everyday life, do not produce such signals. The most frequently met signals are more or less random in nature, and may be considered as broad-band or narrow band noise, or various combinations of both types.

For the description of such processes the existing theory for harmonic signals is not directly applicable because a random signal cannot be exactly defined analytically in the time domain. To be able to furnish some sort of analytical description we have to apply principles commonly used in theoretical statistics. In previous Brüel & Kjær publications (L 1, L 2) such principles have been discussed to a certain extent, e.g. the use of probability distributions for signal amplitudes, power spectral density functions and auto-correlation functions. The two last mentioned functions (the power spectral density function and the

auto-correlation function) express the signal power properties. This information will, in many cases, suffice, its "disadvantage" being, however, the lack of phase information necessary to solve various problems of interference, reflection or parallel path propagation.

To solve these problems it is necessary to introduce slightly more complex correlation functions or power spectral density functions which, on the average, describe the mutual statistical dependency of two signals, i.e. cross correlation functions or cross power spectral density functions.

Considering that it is common engineering practice today to describe acoustical and mechanical signals in the frequency domain rather than in the time domain the remaining part of this article will discuss the theory and measurement of *the cross power spectral density function*.

2. The Concept of Cross Power Spectral Density

In the publication (L 2) the power spectral density function was defined as

$$W_{xx}(f) = \lim_{B \rightarrow 0} \lim_{T \rightarrow \infty} \frac{1}{BT} \int_0^T x_B^2(f, t) dt \quad /1/$$

showing that the power spectral density, $W_{xx}(f)$, at a frequency, f , is given by the average of the square of that part of the signal time function, $x(t)$ which is contained in an infinitely narrow frequency band, B , centered at the frequency f . The value is averaged over an infinitely long time, T .

Similarly we can define the power spectral density $W_{yy}(f)$ of the signal time function, $y(t)$, by substituting $y_B^2(f, t)$ in the above expression.

Provided that we shall be interested in the so-called cross power spectral density of the signal time functions $x(t)$ and $y(t)$, it is necessary to substitute the square of one of the two signals by their product in the expression /1/.

This substitution results in the definition:

$$W_{xy}(f) = \lim_{B \rightarrow 0} \lim_{T \rightarrow \infty} \frac{1}{BT} \int_0^T x_B(f, t) y_B(f, t) dt \quad /2/$$

The function $W_{xy}(f)$ is generally a complex number and is often designated as $W_{xy}(j\omega)$ where $\omega = 2\pi f =$ angular frequency. In the publication (L 2) the auto-correlation function was defined as

$$\psi(\tau) = \overline{F(t_1) F(t_1 + \tau)}$$

The definition of the cross correlation function is again analogous and for our signal time function $x(t)$ and $y(t)$ it can be defined as

$$\psi_{xy}(\tau) = \overline{x(t) y(t + \tau)} = \lim_{T \rightarrow \infty} \frac{1}{2T} \int_{-T}^{+T} x(t) y(t + \tau) dt \quad /3/$$

This formula describes that the cross correlation function is an average value of the product of the signal time functions $x(t)$ and $x(y)$, the latter being delayed by the time τ .

According to the Wiener-Kintchine relation, also mentioned in (L 2), the cross power spectral density function can be derived from the cross correlation function in that

$$W_{xy}(j\omega) = \int_{-\infty}^{\infty} \psi_{xy}(\tau) \exp(-j\omega\tau) d\tau \quad /4/$$

In the following discussion we shall principally use this definition. The expression /2/ served only to explain the relationship between the terms "cross power spectral density" and "power spectral density" as defined in (L 2).

3. The Approximative Cross Power Spectrometer Principle

Consider first a linear system with one input signal and one output signal, see

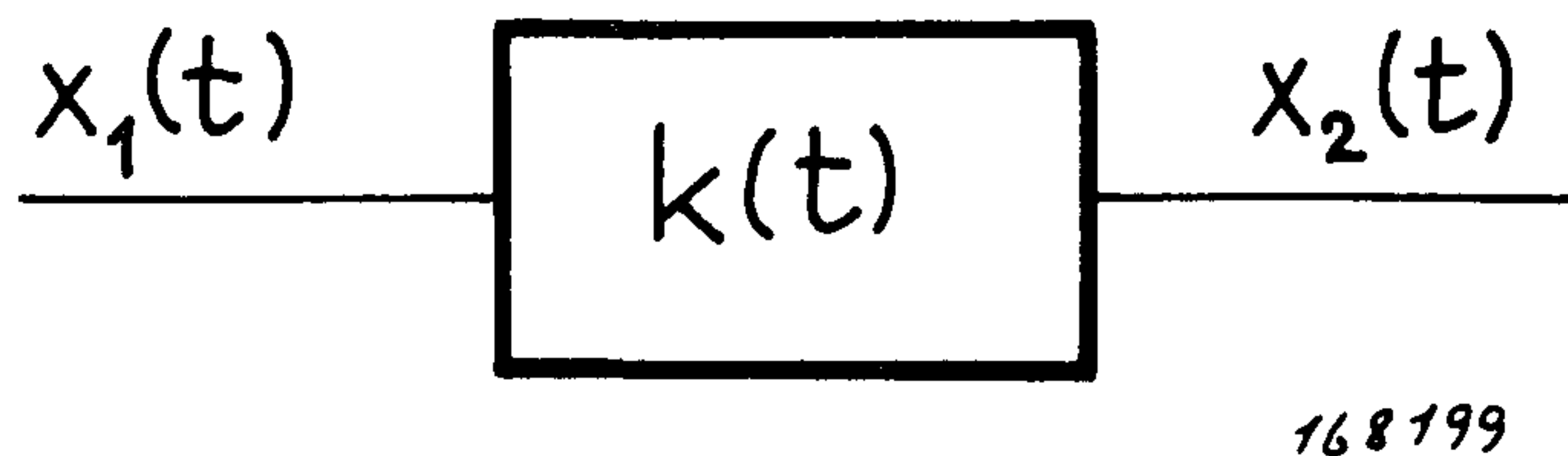


Fig. 1. A linear system with impulse response function $k(t)$ to which the input signal $x_1(t)$ is applied.

Fig. 1. The passage of the signal through the linear system can be expressed in the time domain by the so-called convolution integral

$$x_2(t) = \int_{-\infty}^{\infty} k(\tau) x_1(t-\tau) dt \quad /5/$$

where $k(t)$ = unit impulse response of the linear network

$x_1(t)$ = input signal

$x_2(t)$ = output signal

τ = independent time variable

Consider next Fig. 2. The signal $x(t)$ is passed through the network K with a unit impulse response, $k(t)$, and the signal $y(t)$ through the network H with a unit impulse response, $h(t)$, both output signals being multiplied and the

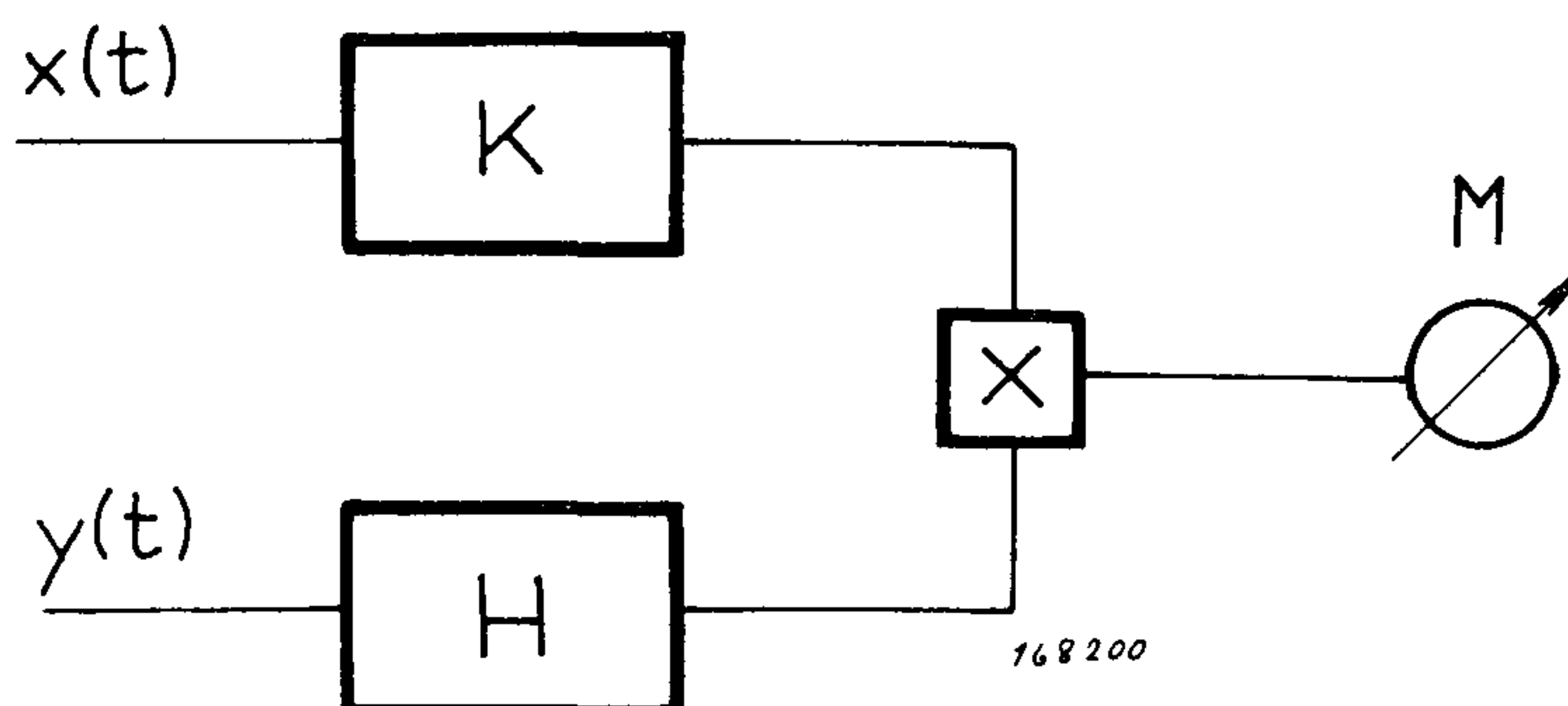


Fig. 2. The principle of cross-power measurements.

average value of the product being measured. The result of the measurement will be designated as M^2 and expressed mathematically as

$$M^2 = \overline{x_2(t) y_2(t)} = \lim_{T \rightarrow \infty} \frac{1}{2T} \int_{-T}^T \left[\int_{-\infty}^{\infty} \int_{-\infty}^{\infty} x(t-\tau) k(\tau) y(t-\xi) h(\xi) d\tau d\xi \right] dt \quad /6/$$

where τ and ξ are independent time variables.

As we are dealing with linear theory and physically realizable systems it is possible to interchange the order of separate operations whereafter some mathematical rearrangement, equation /6/ takes the form

$$M^2 = \int_{-\infty}^{\infty} \int_{-\infty}^{\infty} k(\xi + \tau) h(\xi) \left[\lim_{T \rightarrow \infty} \frac{1}{2T} \int_{-T+\xi}^{T+\xi} x(t) y(t + \tau) dt \right] d\tau d\xi \quad /7/$$

The expression in square brackets is identical to the right hand side of equation /3/, whereby

$$M^2 = \int_{-\infty}^{\infty} \int_{-\infty}^{\infty} k(\xi + \tau) h(\xi) \psi_{xy}(\tau) d\xi d\tau \quad /8/$$

It can be proved that

$$\int_{-\infty}^{\infty} k(t + \xi) h(\xi) d\xi = \int_{-\infty}^{\infty} K^*(j\omega) H(j\omega) \exp(-j\omega\tau) df \quad /9/$$

where

$$H(j\omega) = \int_{-\infty}^{\infty} h(\xi) \exp(-j\omega\xi) d\xi \quad /10a/$$

$H(j\omega)$ is the transfer function for the network H in the frequency domain and

$$K^*(j\omega) = \int_{-\infty}^{\infty} k(\tau) \exp(j\omega\tau) d\tau \quad /10b/$$

$K^*(j\omega)$ is the complex conjugate function to the system transfer function $K(j\omega)$ for the network K .

Substituting the expression /9/ in equation /8/ gives after rearranging the terms

$$M^2 = \int_{-\infty}^{\infty} K^*(j\omega) H(j\omega) \left[\int_{-\infty}^{\infty} \psi_{xy}(\tau) \exp(-j\omega\tau) d\tau \right] df \quad /11/$$

where the expression in square brackets is identical with equation /4/, i.e. the cross power spectral density function. The resulting form of the equation is thus

$$M^2 = \int_{-\infty}^{\infty} W_{xy}(j\omega) K^*(j\omega) H(j\omega) df \quad /12/$$

In carrying out further derivations let us assume that both the networks K and H have the properties of idealized bandpass filters, satisfying the relations

$$K^* (j\omega) H (j\omega) = \begin{cases} 1 & \text{for } f_d \leq f \leq f_h \\ 0 & \text{for } f < f_d; f > f_h \end{cases} \quad /13/$$

where f_d and f_h are the limiting frequencies of the band-pass filters. A quantity $M_1^2(f)$ can then be defined as

$$M_1^2 (f) = \int_{f_d}^{f_h} \text{Re} \{ W_{xy} (j\omega) \} df \quad /14/$$

where $\text{Re} \{ W_{xy} (j\omega) \}$ is the real part of the cross power spectral density function. If the idealized band-pass filters have such a configuration that the following relations are satisfied

$$K^* (j\omega) H (j\omega) = \begin{cases} -j = -\sqrt{-1} & \text{for } f_d \leq f \leq f_h \\ 0 & \text{for } f < f_d; f > f_h \end{cases} \quad /15/$$

it can be proved that

$$M_2^2 (f) = \int_{f_d}^{f_h} \text{Im} \{ W_{xy} (j\omega) \} df \quad /16/$$

where

$$W_{xy} (j\omega) = \frac{1}{B} [M_1^2 (f) + jM_2^2 (f)] \quad /17/$$

$$B = f_h - f_d \quad ; \quad f = \sqrt{f_h \times f_d}$$

provided that the variation of $W_{xy} (j\omega)$ is small inside the frequency band, B , considered.

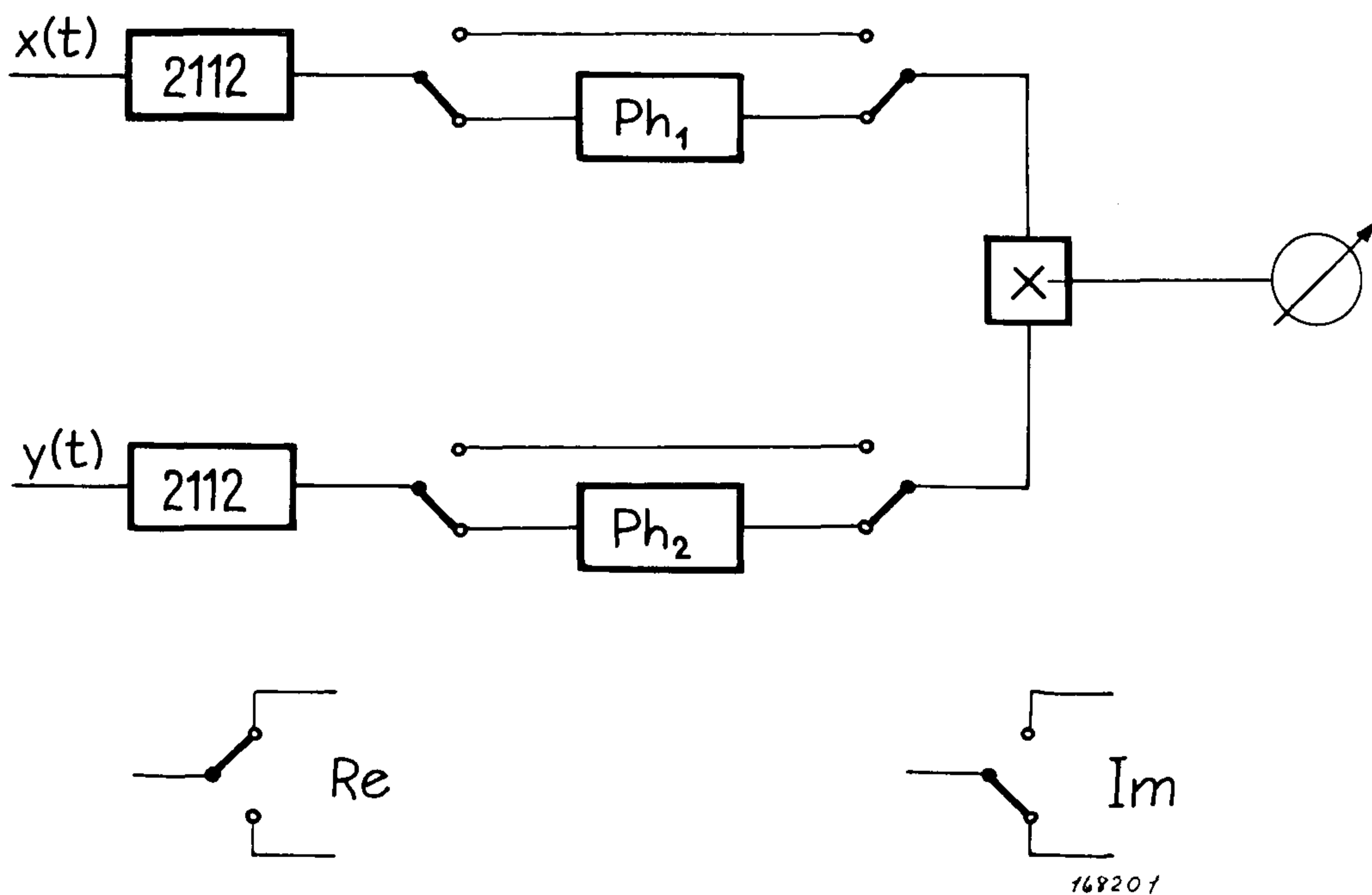
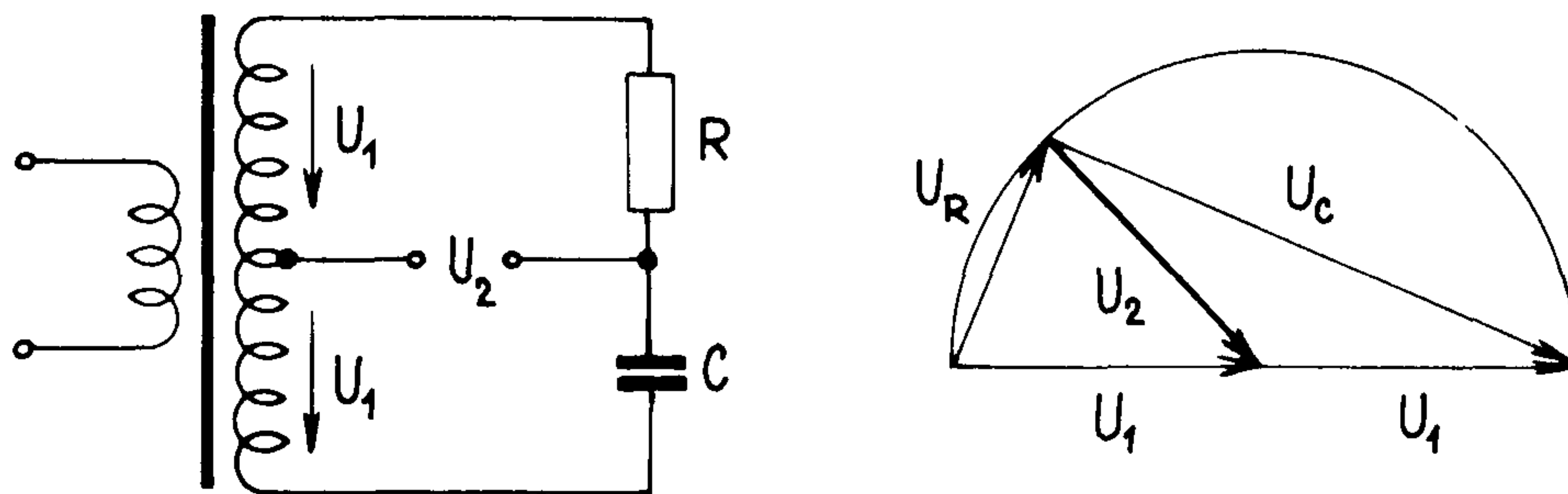


Fig. 3. A cross-power spectrometer.

4. Realization of a Cross Power Spectrometer

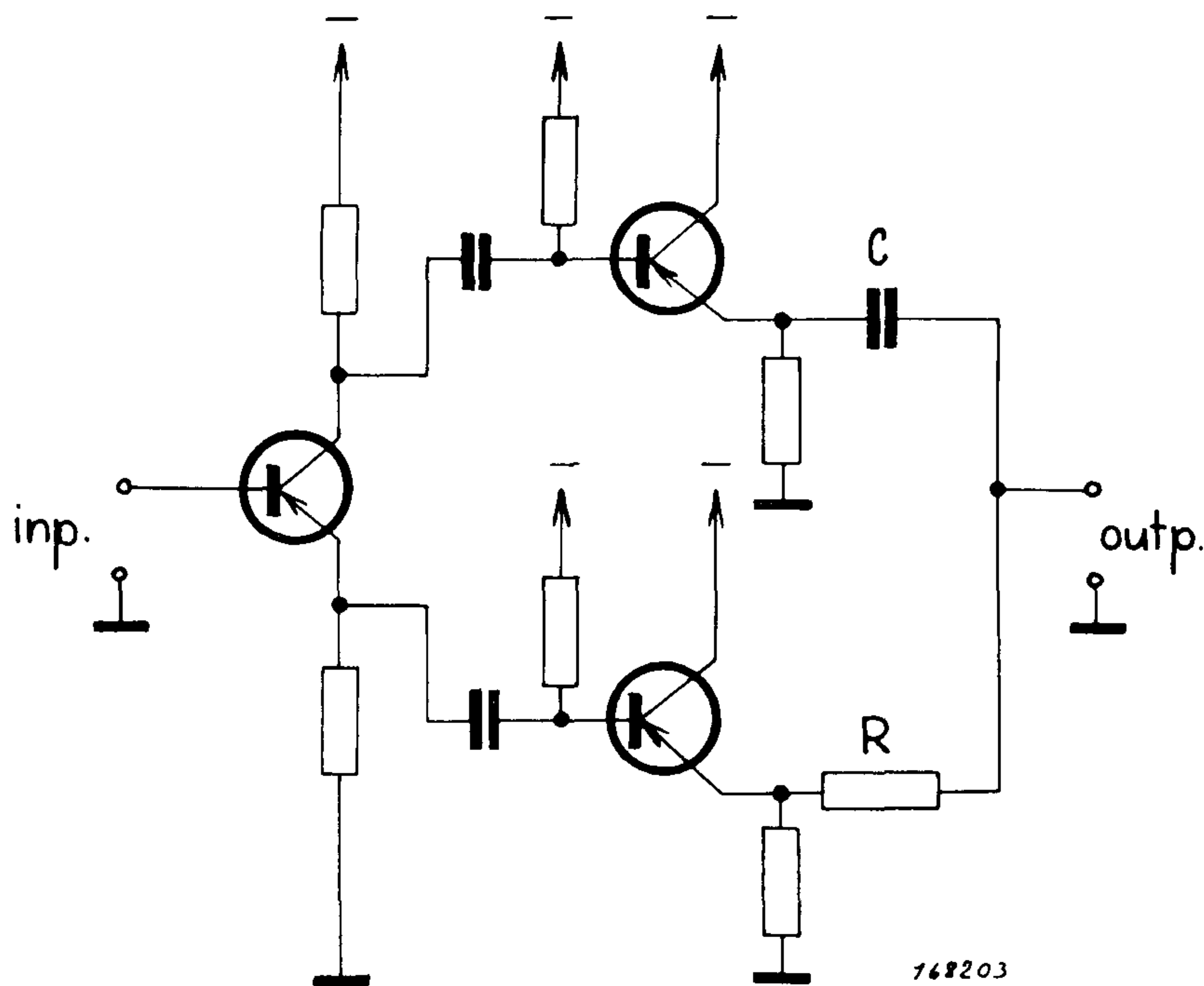
Let us now interpret the practical results of the above theoretical derivations. Equation /13/ is satisfied if both of the filter networks used (K and H) are identical and have unit gain. To produce such networks two B & K Audio Frequency Spectrometers Type 2112 may be used.

Similarly, equation /15/ is satisfied if the output signal from one of the two networks (K and H) is turned 90° ($\pi/2$) in phase. This can be realized in practice by adding two additional networks to the Spectrometers (Ph_1 and Ph_2 in Fig. 3). A further necessary operation is to multiply the output signals, an operation which in our case was performed by means of a DISA Type 55 A 06 correlator. It is clear, however, that any good analog multiplier may be used for this



168202

(a)



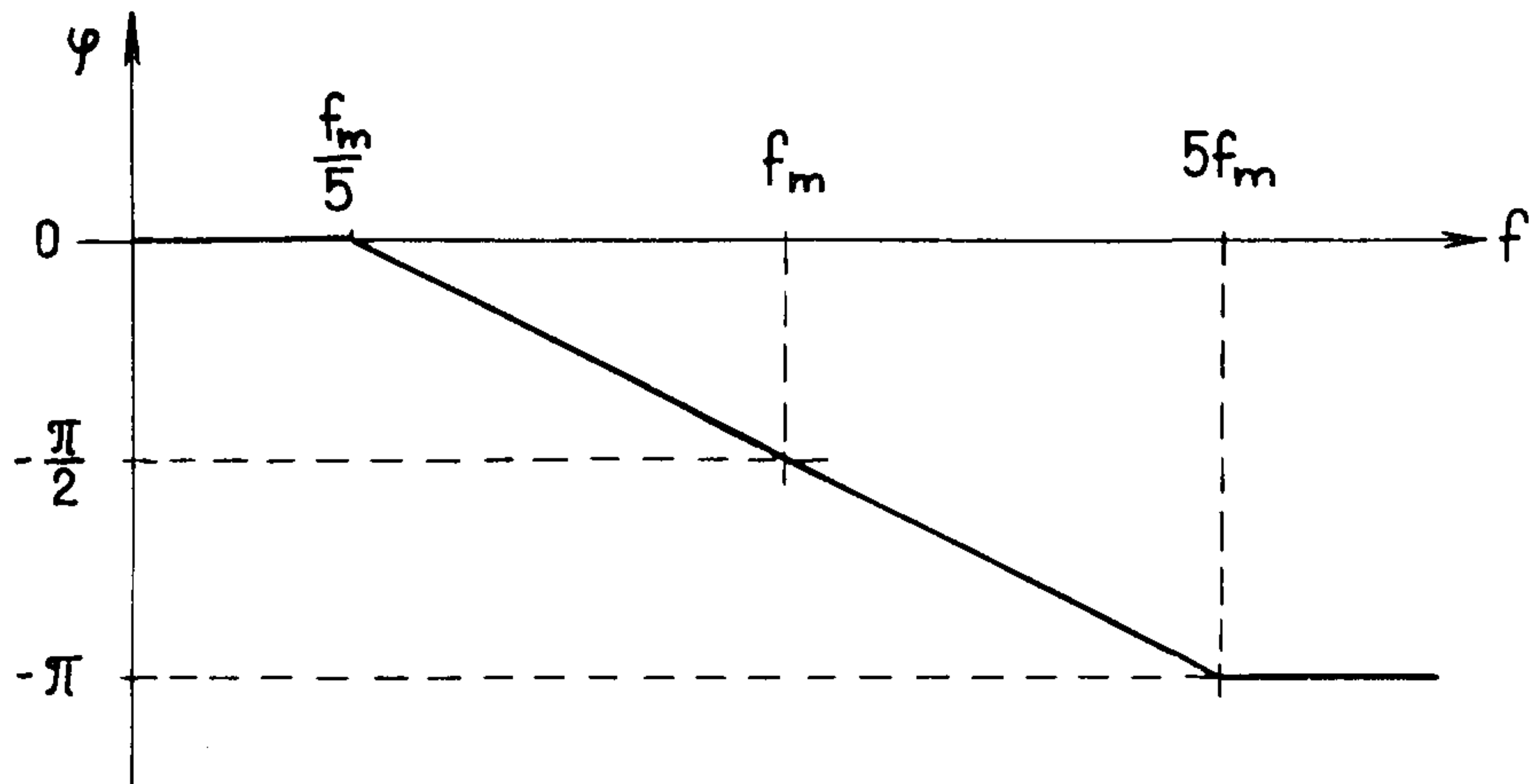
168203

(b)

Fig. 4. The Görge's bridge circuit.
a) Principle of operation.
b) Basic schematic diagram.

purpose. The complete measuring arrangement as used in the Motor Car Research Institute in Prague is sketched in Fig. 3.

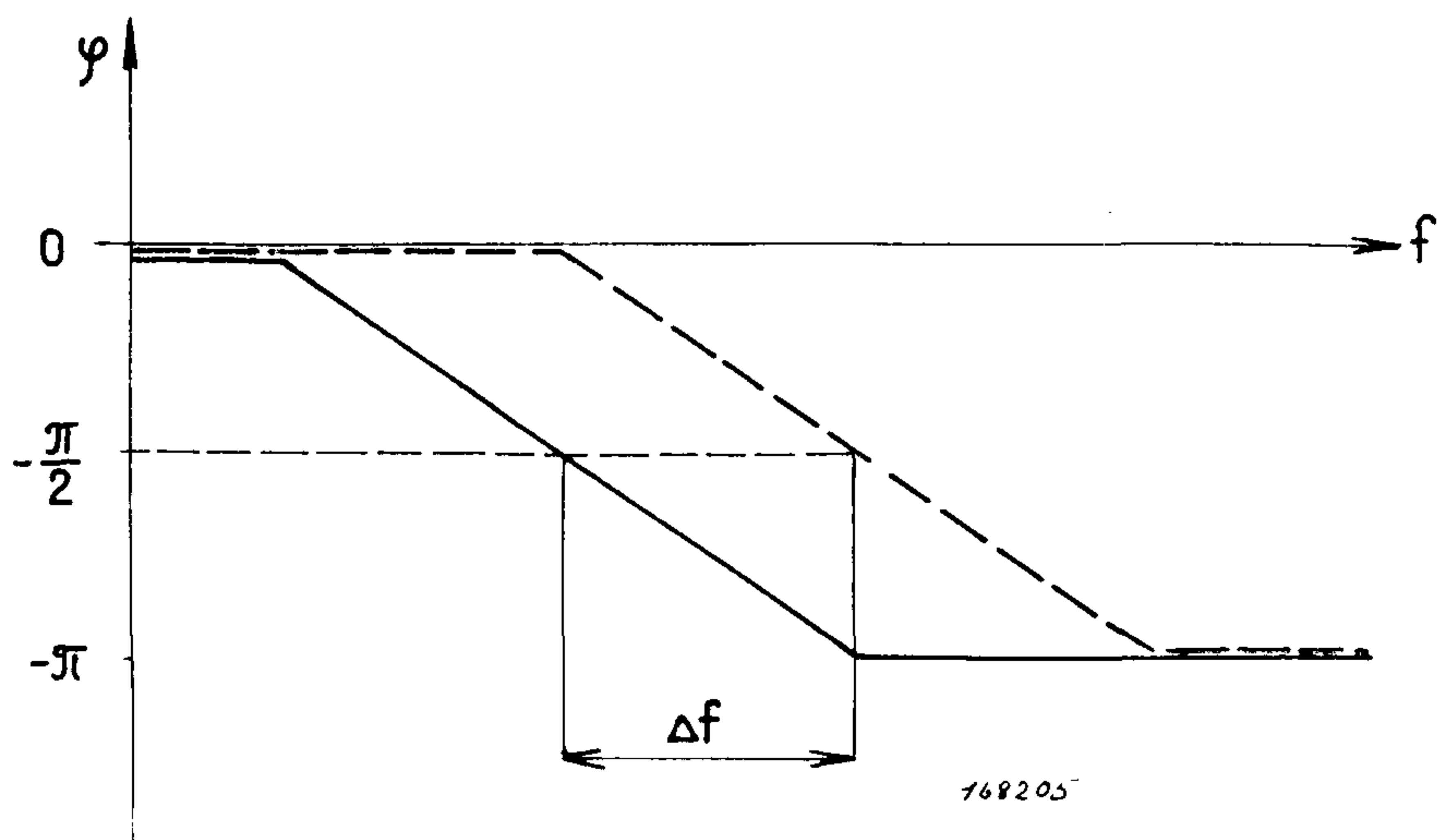
The greatest problem of the cross-power spectrometer arrangement shown is to provide the required phase shift of 90° ($\pi/2$) over the complete frequency band of the band-pass filters in the Spectrometers. In the authors construction the use of two so-called Gørges bridges, the principle of which is shown in Fig. 4a), proved to be the best solution to this problem. The actual circuit connections are sketched in Fig. 4b).



168204

Fig. 5. Theoretical phase vs. frequency response of a Gørges phasing network.

Fig. 5 shows the phase vs. frequency characteristic of one of the bridges, its amplitude transmission characteristic being frequency independent. By suitable choice of components in the networks Ph_1 and Ph_2 (Fig. 3) the relative phase angle between the two outputs can be kept at a value of 90° ($\pi/2$) inside the frequency band, Δf , see Fig. 6.



168205

Fig. 6. Theoretical phase vs. frequency characteristics of two Gørges phasing networks ensuring a constant phase difference between the outputs of 90° ($\pi/2$).

The instrumentation system described above has been developed by the authors in the Motor Car Research Institute in Prague and has been used to solve a number of problems, some of which are briefly mentioned in the following.

5. Some Uses of the Cross-Power Spectrometer

By means of the spectral theory of random signals a series of problems can be solved. Some of these will be discussed in conjunction with Part II of this paper while a particularly important application of cross-power spectral measurements is described below. This is its use to determine the properties of linear systems with a non-deterministic input.

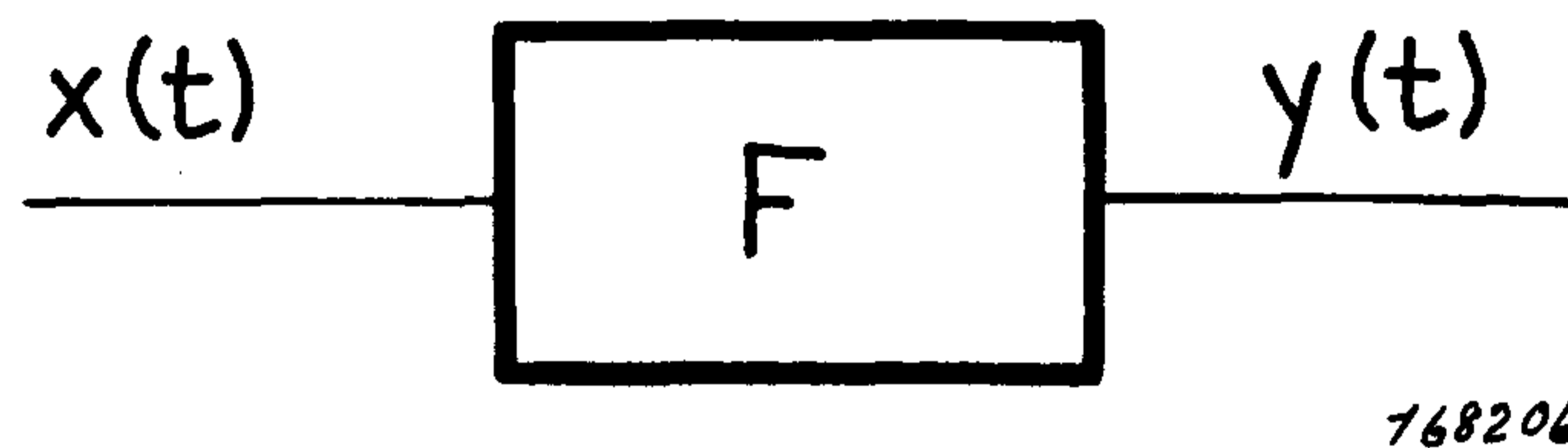


Fig. 7. A linear system with input $x(t)$ and output $y(t)$.

Let the (random) signal $x(t)$ be applied to the input of an unknown linear system with a complex transfer characteristic $F(j\omega)$, see Fig. 7. The output from the system is designated as $y(t)$. It can now be shown theoretically that the cross-power spectral density function of the input signal, $x(t)$, and the output signal, $y(t)$, is related to the power spectral density function of the input signal by the relationship

$$W_{xy}(j\omega) = F(j\omega) W_{xx}(j\omega) \quad /18/$$

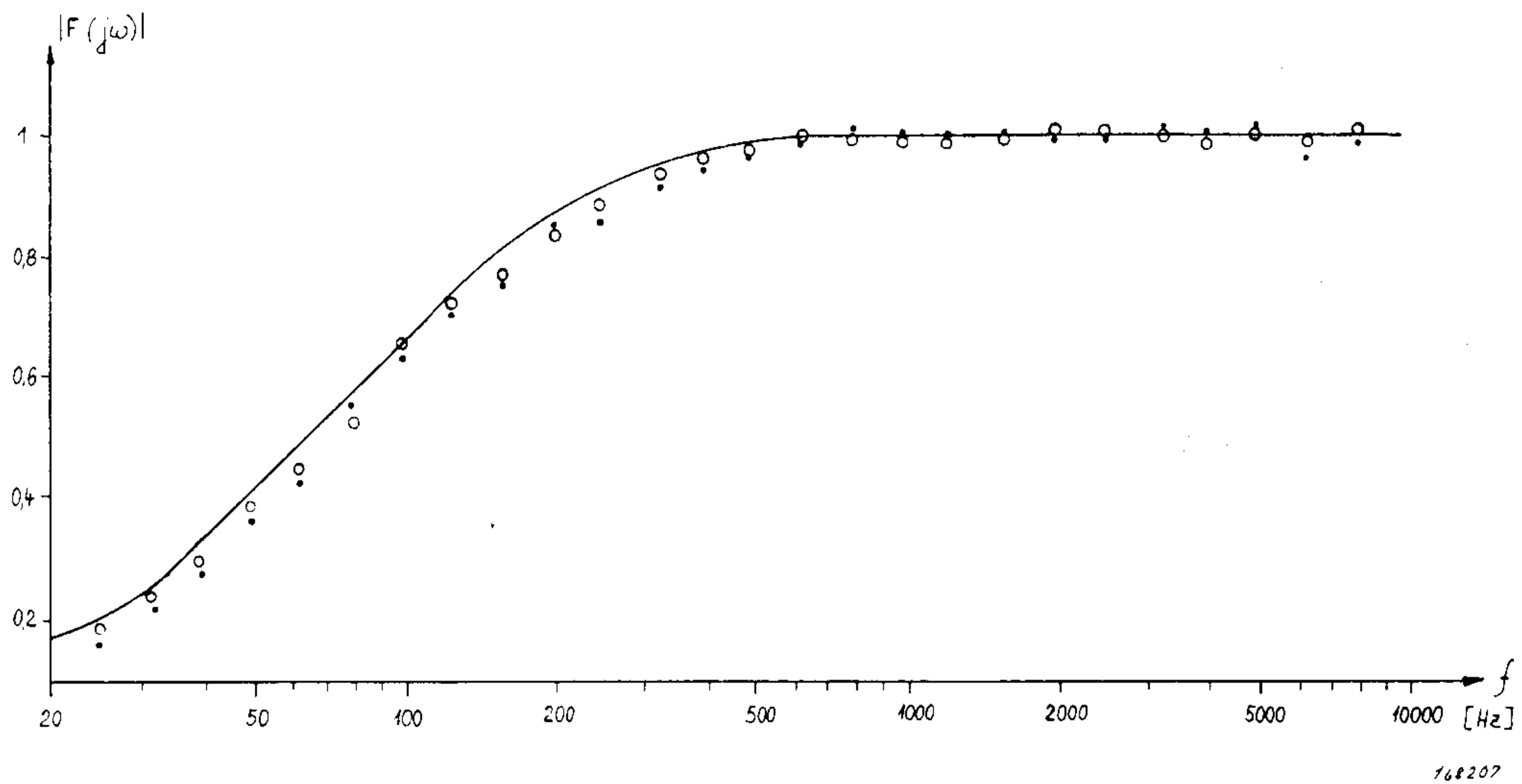
where $W_{xx}(j\omega)$ = power spectral density of the input signal.

$W_{xy}(j\omega)$ = cross power spectral density of the output and input signals.

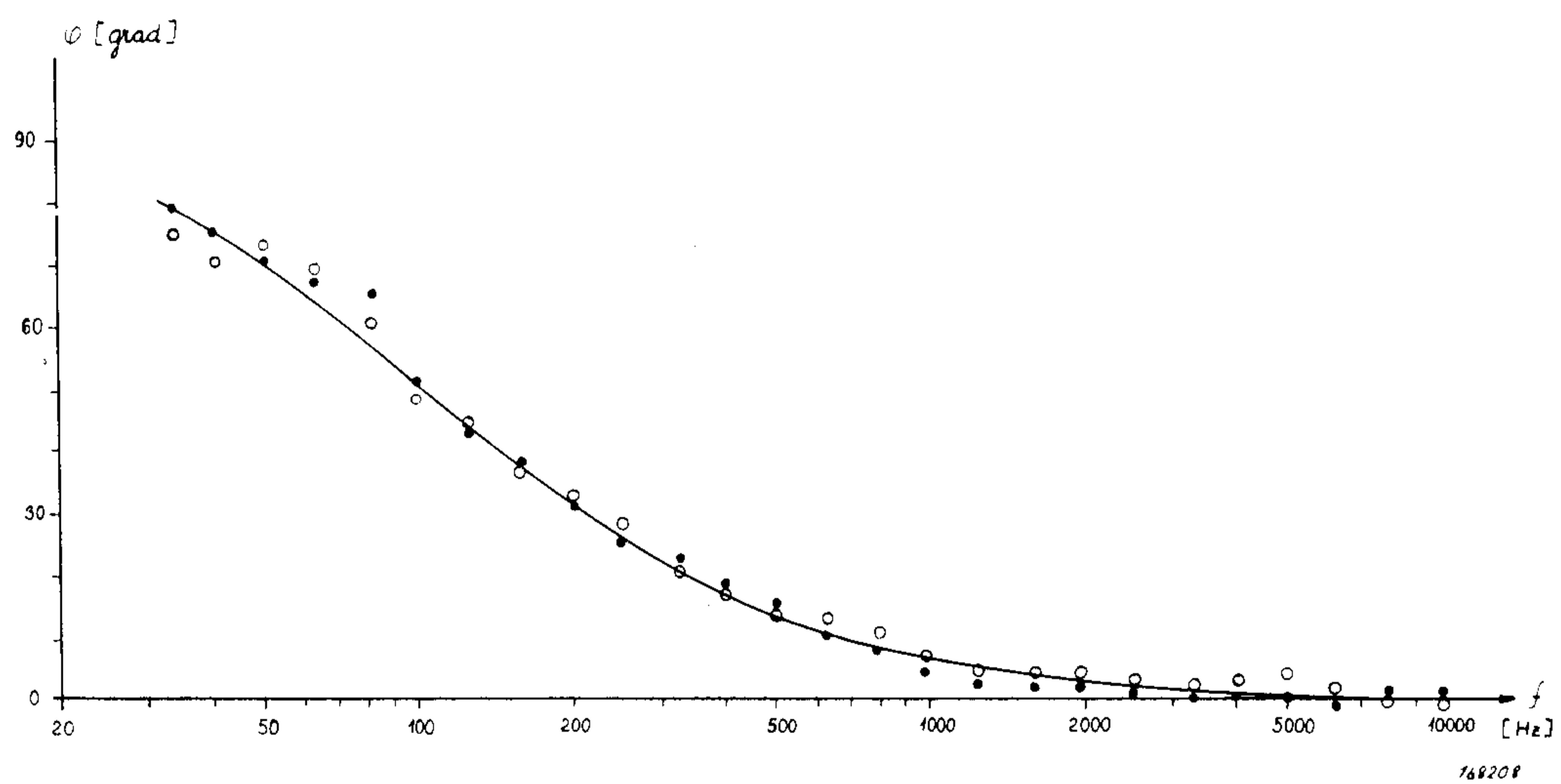
The application of the instrumentation system, described in the preceding text, to the above problem can be illustrated by the following:

The input and output signals of the system, Fig. 7, can be measured. However, let us assume that the input signal to the system cannot be freely chosen but is of random nature. It is then possible from measurements in conjunction with formula /18/ to determine the transfer characteristic of the system.

As an example of such measurements the amplitude and phase characteristics of a known RC-network are shown in Fig. 8 together with some measured points. In the first case the characteristics were measured by applying white Gaussian random noise from a Random Noise Generator Type 1402 to the input of the system (measurement points marked by \circ). In the second case the input was obtained from tape recorded automotive noise (measurement points marked by \bullet). The agreement between the theoretically calculated response and the measured data is quite satisfactory. In Fig. 9 the same data is plotted in the complex plane.



(a)



(b)

Fig. 8. Transmission characteristic of an RC-network.

a) Amplitude characteristic.

b) Phase characteristic.

○ = *Measured with white Gaussian random noise applied to the input.*

● = *Measured with tape recorded automotive noise applied to the input.*

The result of a second example of cross-power spectrum measurements is shown in Fig. 10. Here the vibration transmission through an elastic bearing member of an automotive engine was measured. In this case the input signal was obtained from the vibrations of a running engine.

6. Conclusion

The methods of modern statistical dynamics enable us to solve numerous problems connected with random noise and vibration phenomena. These methods can, however, normally be utilized only in conjunction with highly

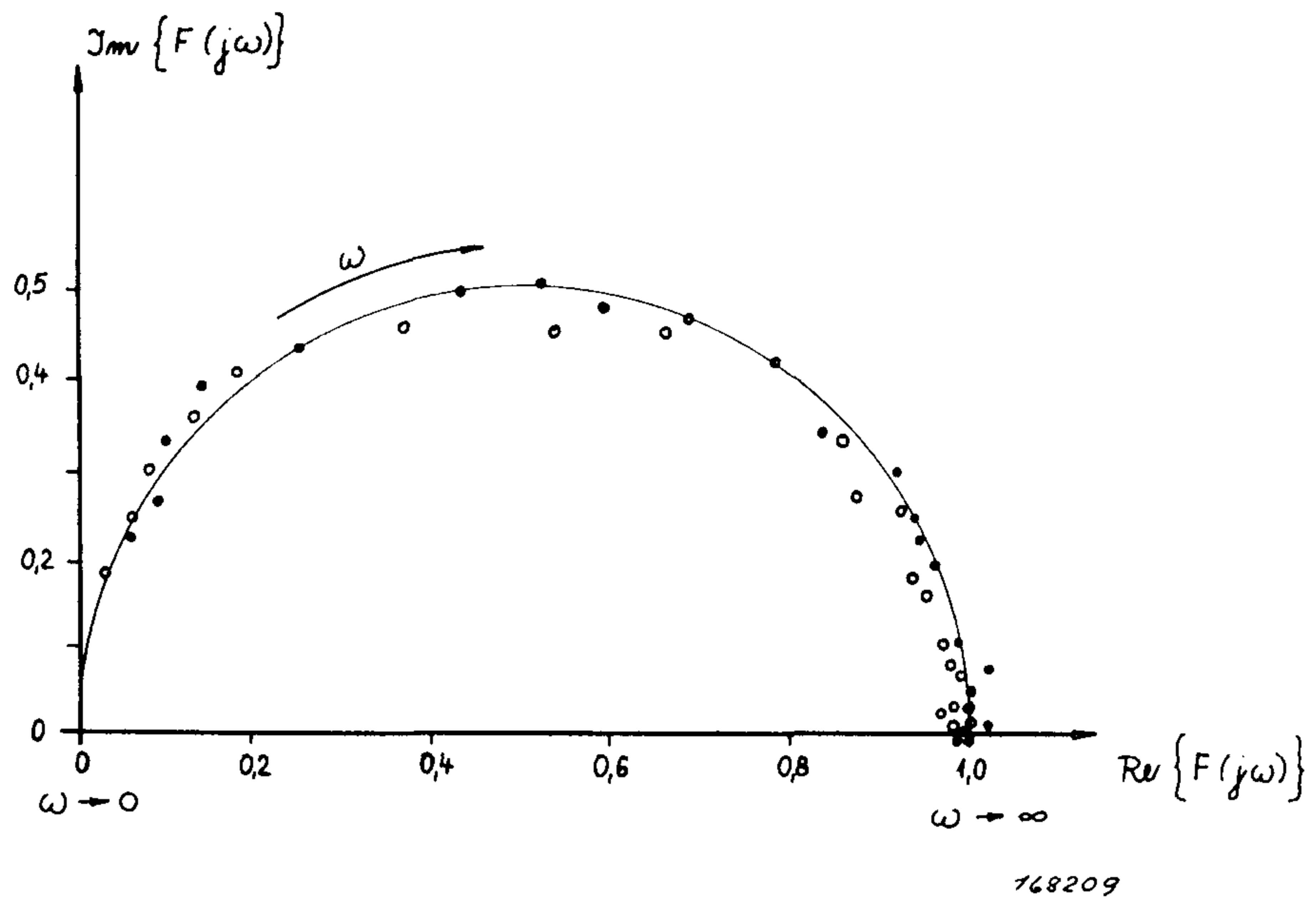


Fig. 9. The same data as shown in Fig. 8 replotted in the complex plane.

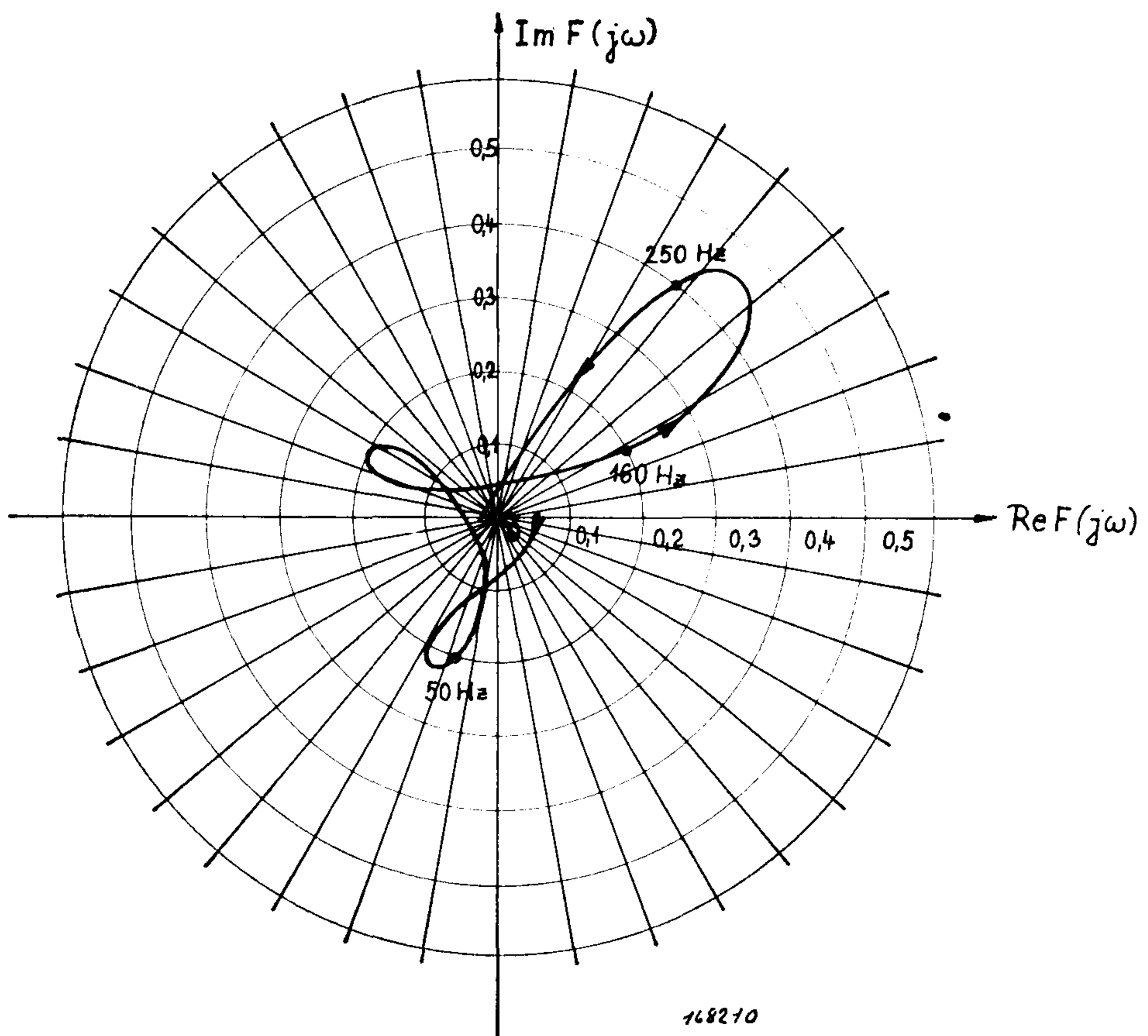


Fig. 10. Results of vibration transmission measurements on an elastic bearing member of an automotive engine plotted in the complex plane.

specialized expensive measurement equipment. On the other hand, as illustrated in this article some problems can be solved by means of analog instrumentation systems currently used in modern laboratories.

One of the greatest limitations of the instrumentation system discussed here is that its smallest filter bandwidth is 1/3 octave. This bandwidth may be too large to solve many of the existing problems, and filters with narrower bandwidths have to be used*). An instrument with considerably narrower bandwidth which is presently available on the market is the Frequency Analyzer Type 2107. It is, however, not immediately possible to apply the principles discussed in this article to the Type 2107 Analyzer because identical phase characteristics of the band-pass filters cannot be guaranteed with tuned analyzers. In the Motor Car Research Institute in Prague a method has been developed which allows cross-power spectral measurements to be made also with this instrument. The method used will be discussed in Part II of this paper.

Literature

- /L 1/ Jens T. Broch "Automatic Recording of Amplitude Density Curves", Brüel & Kjær Technical Review, Nr. 4 - 1959.
- /L 2/ "Application of B & K Equipment to Frequency Analysis and Power Spectral Density Measurements", B & K Publication, 1966.
- /L 3/ W. B. Davenport, W. L. Root "An Introduction to the Theory of Random Signals and Noise", McGraw Hill, New York, 1958.
- /L 4/ E. Skudrzyk "Die Grundlagen der Akustik", Springer-Verlag, Wien 1954.
- /L 5/ L. L. Beranek "Acoustic Measurements", John Wiley & Sons, 1949.
- /L 6/ F. H. Lange "Korrelationselektronik", VEB-Verlag Technik, Berlin, 1959.

*) Editor's note: A system with very narrow bandwidth is discussed in the preceding article.

News from the Factory

Piezoelectric Accelerometers Type 4339 and 4343

These Accelerometers, which are designed as single-ended compression type accelerometers, can be used even in extreme environments. An extension calibration and temperature stabilizing procedure has been undertaken to ensure completely predictable performance and stable operation, one of the main features being that each accelerometer of one type has exactly the same sensitivity (to within $\pm 2\%$). The accelerometer housing is of an all welded stainless steel construction which makes it absolutely waterproof. A special ceramic input socket ensures complete sealing even after repeated temperature cycling up to 250°C.

Some typical performance data are summarized below

<i>Accelerometer</i>	4339	4343
Contained in set as Type	4319	4323
Contained in package of 5 as Type	4359	4363
Sensitivity mV/g	10 ± 0.2	approx. 10
Sensitivity pC/g	approx. 10	10 ± 0.2
Free resonance kHz	75	75
Capacity incl. cable pF	1000	1000
Transverse sensitivity %	< 3	< 3
Max. ambient temp. °C	260	260
Temperature sensitivity dB/°C	0.02	0.02
Max. shock, g	10,000	10,000
Freq. range with steel screw $\pm 2\%$ Hz	$0.5^* < -10,000$	$0.5^* < -10,000$
on stainless steel $\pm 10\%$	$0.5^* < -15,000$	$0.5^* < -15,000$
Weight, grams/ounces	16/0,57	16/0,57
Sensitivity time stability	2 % per year	2 % per year

Each Accelerometer is supplied with its individual calibration chart and an instruction manual containing a number of additional typical characteristics and operating instructions.

Miniature Piezoelectric Accelerometer Type 4344

The miniature Accelerometer Type 4344 is designed for vibration measurement on light-weight structures where a heavy transducer would change the mode of vibration and thereby invalidate the results obtained. It will be found



Fig. 1. The Accelerometer Set Type 4359 containing the Accelerometer Type 4339.

valuable in research projects involving thin plates and shells, such as aircraft skins, car bodies, component testing etc.

This Accelerometer is also of the single-ended compression type. The construction is sealed and waterproof for operation in moisture chambers or

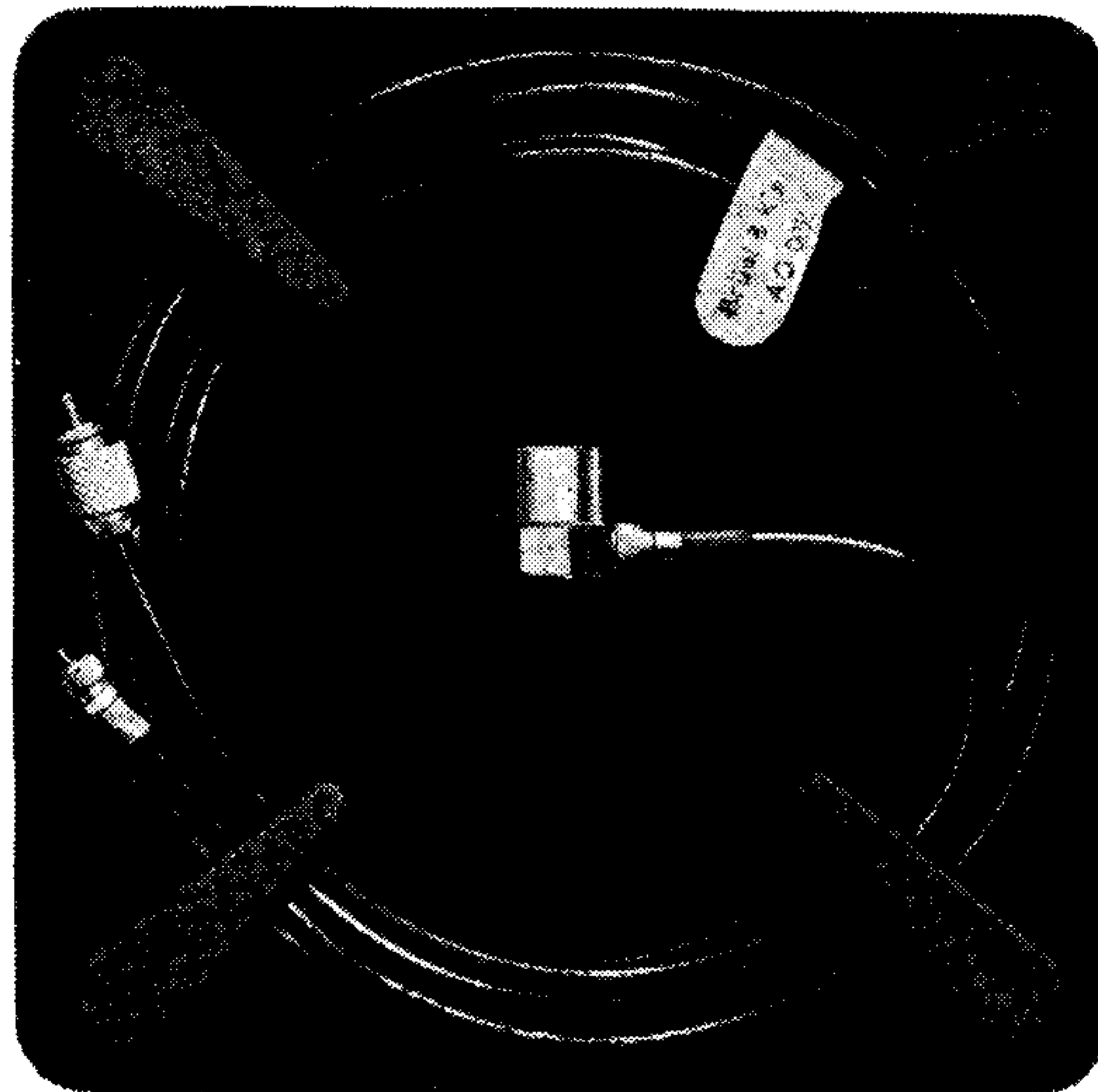


Fig. 2. Single unit of an Accelerometer Package of 5, Type 4364, containing Accelerometer Type 4344.

under water, and the working temperature range is from -90 to $+260^{\circ}\text{C}$. Each Accelerometer is supplied with its individual calibration chart and some typical performance data are summarized in the table below.

Accelerometer	4344	* Transverse Sensitiv. %	8
Contained in set as Type	4324	Max. Ambient Temperature ($^{\circ}\text{C}$)	260
Contained in package of 5 as Type	4364		0.02
* Sensitivity (mV/g)	2-3	* Freq. Range (Hz) 2% 10%	0.5-25,000 0.5-40,000
* Charge Sensitivity (pC/g)	2-3	Weight (grams)	2
* Free Resonance (kHz)	125	Material of Base	Titanium
* Capacity includ. cable (pF) **	900	* The low frequency cut-off is determined by preamplifier.	
* Individual values given on the calibration chart. ** With standard low-noise cable, 1.2 m (4 feet) long.			

Wide Range Charge Amplifier Type 2624

The combination of a charge amplifier and a piezoelectric accelerometer gives a sensitivity which is independent of the cable length within very wide limits. This makes a charge amplifier especially attractive in vibration systems where different cables are used. The Charge Amplifier Type 2624 may be used with cable lengths up to several thousand metres. A charge amplifier also provides the possibility of very low frequency measurements and in the case of Type 2624, the limit is 0.003 Hz in the least sensitive mode, this makes the pre-amplifier ideal for measurements of shocks and long duration transients. Typical frequency characteristics for various settings of the Charge Amplifier controls are shown below.

Vibration Pick-up Preamplifier Type 2625

The Vibration Pick-up Preamplifier Type 2625 is provided with integration networks for measurement of velocity and displacement in addition to acceleration. There are three input sockets connected to a selector switch with individual sensitivity adjustment for each input. The two inputs not in use are connected to ground.

A function selector controls three different gain ranges for the three inputs: 1. Variable from -40 to -20 dB. 2. Variable from 0 to $+20$ dB. 3. Fixed at 0 dB. The integration networks are passive RC networks with three different lower frequency limits, 1, 10 and 100 Hz for velocity, and six limits. 1, 3, 10, 30, 100 and 300 Hz for displacement measurements.

A field effect transistor stage in the input circuit gives extremely high input

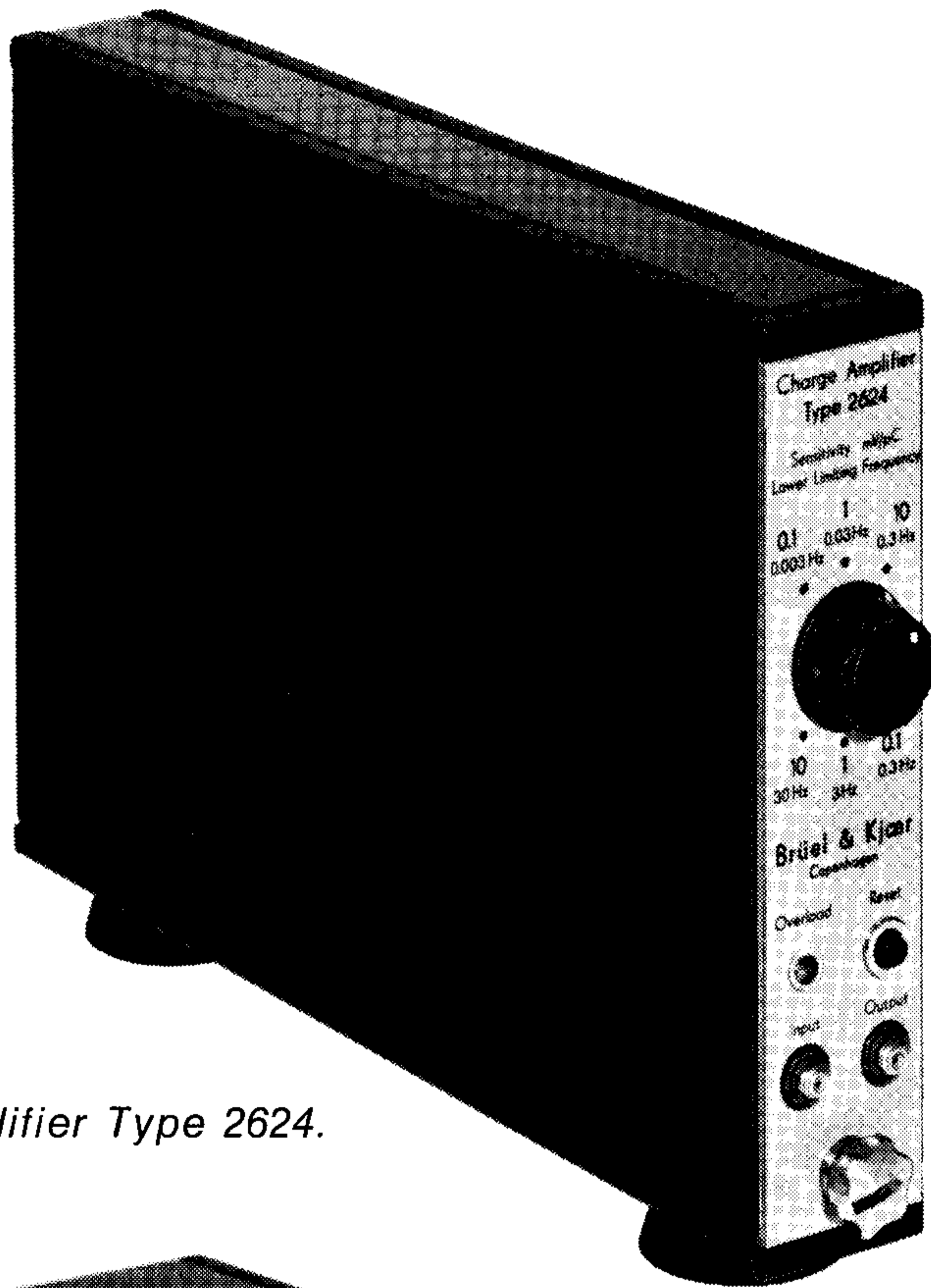


Fig. 3. Charge Amplifier Type 2624.



Fig. 4. Vibration Pick-up Preamplifier Type 2625.

impedance variable from about 3000 M Ω at + 20 dB. To allow for convenient battery operation of the preamplifier, if this should be desired, a special built-in battery compartment is included in the construction. However, the instrument can also be powered by an external source of 28 Volts DC.

New Module System of Instrumentation

Both the Preamplifiers Type 2624 and 2625 (see above) have dimensions which fit the new Brüel & Kjær module system of instrumentation. This system has been designed to allow for a very flexible mechanical system build-up, and the instruments can be mounted in portable, transportable or permanent configurations as follows:

1. As single instruments (2624, 2625).
2. One-tier system in various combinations of sizes. – In metal cabinet, metal cabinet in mahogany housing or metal cabinet for rack mounting, corresponding to our normal A, B or C versions.
3. Three-tier system in various combinations of sizes.

Any necessary instrument service has been made as simple as possible so far as case disassembly is concerned, as the construction is made up of slide-on and off panels requiring the minimum of retaining screws.

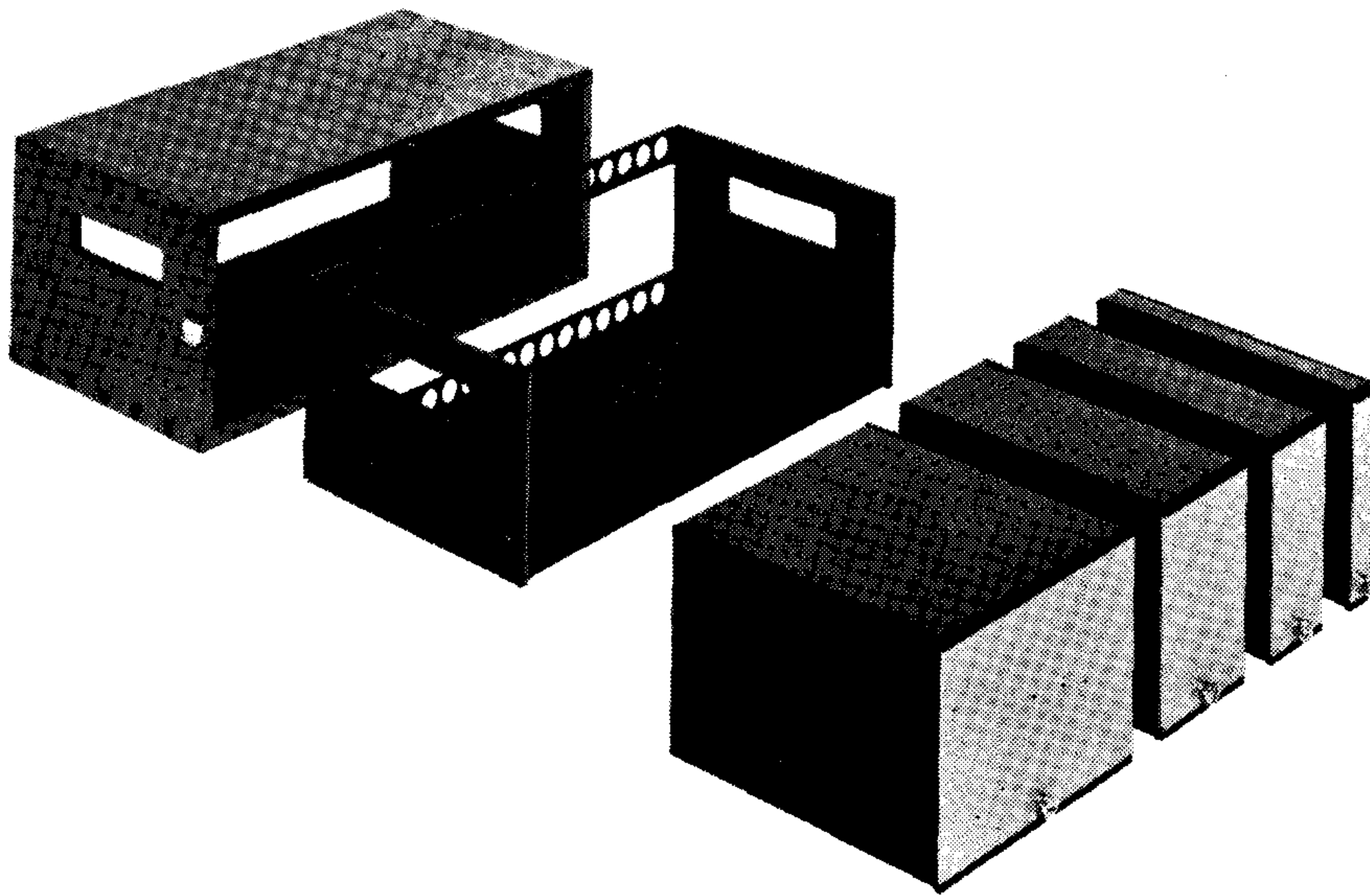


Fig. 5. One-tier Module System of Instrumentation.

OCT. 1968

Brüel & Kjær

ADR.: BRÜEL & KJÆR
NÆRUM - DENMARK



TELEX 5316

TELEPHONE: 800500
BRUKJA, Copenhagen